

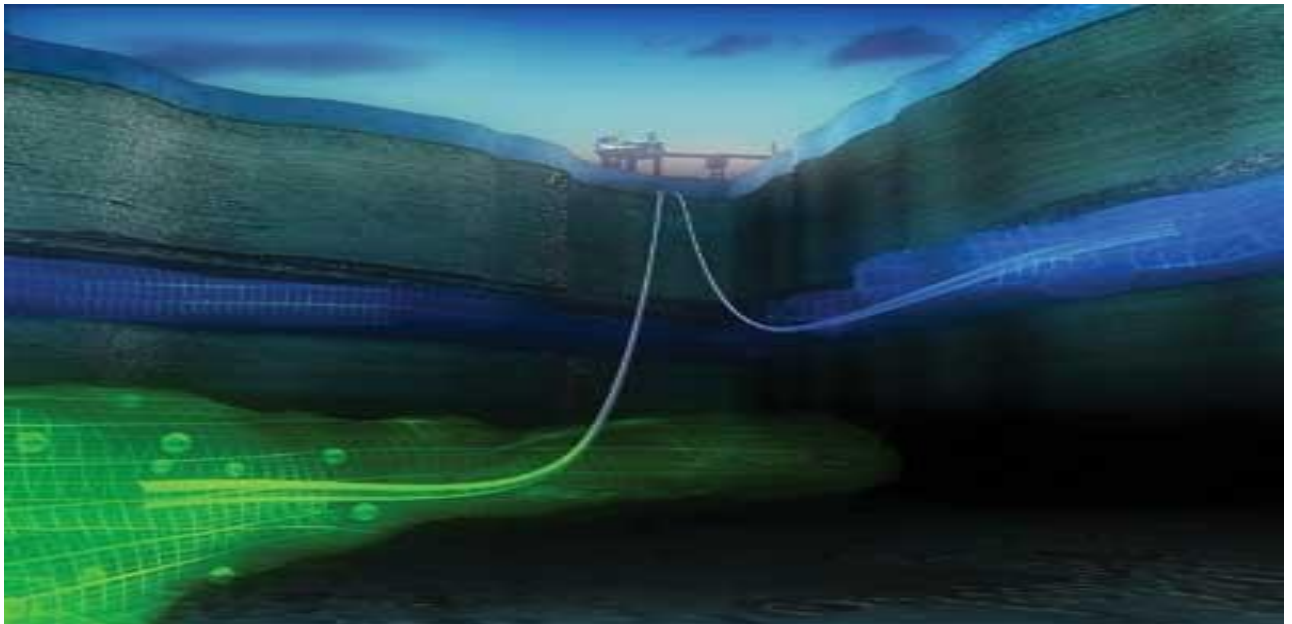
# 2014

Aalborg Universitet Esbjerg

Department of  
Biotechnology, Chemistry  
and Environmental  
Engineering, Section of  
Chemical Engineering

Ms.C. in Oil and Gas  
Technology 2014, 10th  
Semester

# [INVESTIGATION OF EOR METHODS FOR NAGANI OIL FIELD]



**Supervisors:**

Professor Erik Gydesen Søgaard

Muhammad Adeel Nasser Sohal

**Author:**

Petya Vakova

## Abstract

The main objective of this project was the applying and implementation of enhanced oil recovery (EOR) method in the Nagani oil field.

Primarily, the characteristics of the reservoir and their compatibility with different EOR methods are assessed based on the established screening criteria. The resulted selection of appropriate method based on the criteria corroborated for the usage of Polymer Flooding or more specifically polymer-augmented water-flooding. Furthermore, introduction of the analytical approach for estimating the reservoir performance was set, initially in regard to the water-flooding and subsequently for the polymer-augmented water-flooding. This led to critical empirical data revision and calculation procedure, whose outcome was the additional oil recovery evaluation.

The last part of the thesis incorporated the received data and results from the implementation of the polymer-flooding in Nagani oil field. Therein the results regarding the change into the production from the use of water-flooding (Case 1) and polymer-augmented water-flooding (Case 2). This inferred for the corroboration of the most suitable method for the Nagani oil field selection, which process was accomplished with the help of Eclipse Black Oil simulator 2008.1. Moreover, in case to achieve full agreement with the viscosity used in the model, and narrow the ambiguity of the real viscosity of the oil in-situ of the reservoir, two empirical laboratory studies were conducted with the main purpose of visualizing the viscosity change with temperature in isobaric conditions.

### **Project title:**

Investigation of EOR methods for Nagani oil field

### **University:**

Aalborg University, Esbjerg University of Technology- Niels Bohrs Vej 8, 6700 Esbjerg, Denmark

### **Project period:**

10-th semester

### **Submission date:**

13.06.2014

### **Supervisors:**

Professor Erik Gydesen Sogaard

Muhammad Adeel Nasser Sohal

Petya Vakova Signature: \_\_\_\_\_

<sup>1</sup> <http://www.offshore-mag.com/articles/print/volume-71/issue-8/subsea/ior-eor-equipment-moves-toward-seabed.html>

## Acknowledgments

I would like to express my profound gratitude to my supervisors Professor Erik Gydesen Søgaard and Muhammad Adeel Nasser Sohal for their support and guidance throughout the project work.

Also I would like to thank Dorte for guidance during the laboratory experiments, hers fruitful discussions and commitment in the help for achieving accurate results.

## Abbreviations and Nomenclature

$B_o$ – oil formation volume factor – stb/stb	$S_w^*$ - water saturation at the polymer front
$B_{oi}$ – oil FVF at start of flood;	$S_{w1}$ - oil bank water saturation
$c$ – mean curvature of the oil droplet	$S_{w2}$ - water saturation at the production well
$D$ – reservoir depth	$S_{wf}$ – flood-front saturation;
$D_p$ - polymer retention	$S_{wi}$ – initial water saturation;
$E_{AS}$ – areal microscopic displacement efficiency.	$S_{wr}$ – residual water saturation
$e^{bSw}$ – the exponential value of slope ( $b$ ) multiplied with	$T$ – reservoir temperature - <sup>0</sup> F
$E_d$ - Displacement efficiency	$t$ – time (days)
$E_R$ – recovery factor;	$t_{BT}$ – breakthrough time
$E_V$ – microscopic displacement efficiency;	$t_D$ – dimensionless time
$E_{vol}$ – volumetric sweep efficiency;	$T_r$ – reservoir temperature
$E_{VS}$ – vertical microscopic displacement efficiency;	$T_s$ – ambient (surface) temperature
$f_{wf}$ – slope;	$V_p$ –pore volume
$f_{wf}^*$ - slope for the polymer front	$W_{inj}$ - cumulative water injected (bbl)
$f_{iw}$ –fractional flow of water at interstitial water saturation;	$X$ - distance from origin (feet)
$f_w$ – fractional flow of water – dimensionless;	$x_D$ – dimensionless distance from origin.
$f_w^*$ - fractional flow at the polymer front	$\alpha$ – the dip-angle of the layer;
$f_{w1}$ - oil bank fractional flow	$\gamma_o$ – specific gravity of the oil – dimensionless
$f_{wf}$ – fractional flow of water at the flood-front saturation;	$\rho_d$ – density of the displacing fluid kg/m <sup>3</sup> ;
$F_{wo}$ -Water- Oil ratio (WOR) STB/ STB	$\rho_o$ – density of the crude oil – kg/m <sup>3</sup> ;
$g$ – gravity acceleration;	$\rho_o$ – oil density kg/m <sup>3</sup> ;
$h$ –formation thickness	$\rho_w$ – density of the water – kg/m <sup>3</sup> .
$k$ – permeability;	$\phi$ - Porosity;
$K_d$ – effective displacement fluid permeability;	$\sigma$ – interfacial tension of the oil-water interface;
$K_{dr}$ – relative permeability to displacing fluid in the swept zone	$\phi_{IPV}$ – inaccessible pore volume;
$K_o$ – effective oil permeability;	$\phi_e$ – effective inaccessible pore volume
$K_{or}$ – relative permeability to oil in oil zone;	$\bar{S}_{w3}$ – average water saturation for the polymer flood
$N_p$ - Cumulative oil production STB	$\bar{S}_o$ - Average oil saturation at the flood pattern
OOIP – original oil-in-place	$S_{w3}$ – water saturation of the polymer bank;
$P_w$ – pressure of the water	$t_{D1}$ – dimensionless time regarding oil bank;
$P_o$ – pressure of the oil	$t_{D2}$ – dimensionless time regarding water bank.
$q_i = i_w$ – injection rate, bbl/day	$x_{D1}$ – location of the oil bank at the breakthrough
$Q_o$ - oil rate at reservoir conditions, in STB/day	$x_{D3}$ – location of the polymer bank at breakthrough
$Q_w$ - Water rate at reservoir conditions, in STB/day	$\lambda_d = \frac{K_d}{\mu_d}$ – Mobility of the displacing fluid
$S_{iw}$ – interstitial water saturation	$\lambda_o = \frac{K_o}{\mu_o}$ – mobility of the oil
$S_{oi}$ – initial oil saturation at the start of flood	$\mu_d$ – displacing fluid viscosity - cP
$S_{oi}$ – initial oil saturation	$\mu_o$ – oil viscosity - cp;
$S_w$ –water saturation	$\mu_{OD}$ – dead oil viscosity - cP

## Table of content

Abstract .....	1
Acknowledgments .....	2
Abbreviations and Nomenclature .....	3
Introduction.....	5
1. Enhanced Oil Recovery (EOR).....	7
1.1 Screening criteria for EOR methods .....	15
1.2 EOR methods .....	17
1.3 Selection of EOR method.....	18
1.3.1 Polymer flooding .....	24
2. Analytical method for EOR .....	29
2.1 Calculations for waterflooding in a linear system .....	30
2.1.2 Results .....	38
2.2 Calculations for Polymer-Augmented Waterflooding in linear system.....	40
2.2.2 Results .....	45
2.3 Evaluation of the additional oil recovery .....	47
3. Implementation of Polymer-Augmented waterflooding in Nagani oil field.....	50
Conclusion .....	52
Appendix A – Laboratory measurements.....	53
Table of Figures .....	54
Bibliography.....	55

## Introduction

As a result from increasing energy demand and decreasing number of new discovered fields the enhanced oil recovery (EOR) processes has become a solution for increasing the production. Even in the well studied region of North Sea exists the possibility that only one of nine drilled wells will not be “dry” .(API 2010) In order to increase the yield and prolong the production period of the field, oil industry focus on research and development of different EOR processes. Over the past several decades has been developed various EOR methods. Those methods are necessary for recovering the oil which was left behind due to the conventional methods (primary and secondary recovery).

Before implementing EOR methods it is needed to be made a pre-assessment plan to evaluate, either the quantities are satisfying and the reservoir is worth developing. This is done by assessment wells, which investigates the economical profitability of the reserves. If observed the lack of natural drive then secondary and EOR techniques are needed to be applied. Regarding the production, oil and gas fields’ lifetime often includes four main sections:

- Increasing production;
- Plateau stage – production is relatively stable;
- Decrease in the production;
- Implementation of secondary recovery and EOR methods – supports and leads to final peak of production.

Life cycle of a reservoir is created and presented by U.S. geologist M. King Hubbert on the figure bellow.

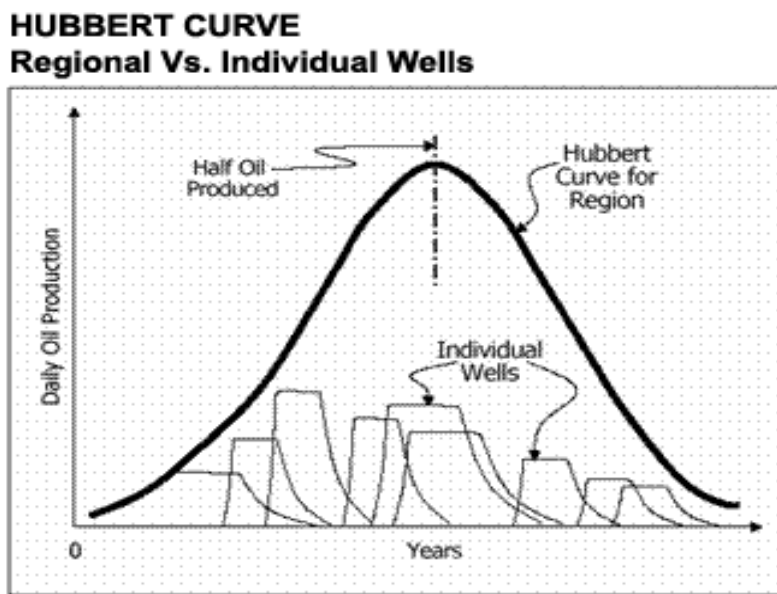


Fig. 1 Hubbert curve (1)

Hubbert curve is a theoretical interpretation of the production life of the field which is fully hypothetical designed and does not refer to all fields. There is no production field which can fit perfectly to the bell shaped curve because the production is based on the different parameter and depends on the various factors. Nevertheless, Hubbert curve is an important predictive tool.

Model of global oil and gas production which is observed on Fig.2 is based on real values. The model describes a reached pick of conventional oil and gas production in present days. According to different scenario calculated and depicted is that the pick has occurred in 2008 (*World Energy Outlook of 2010*).

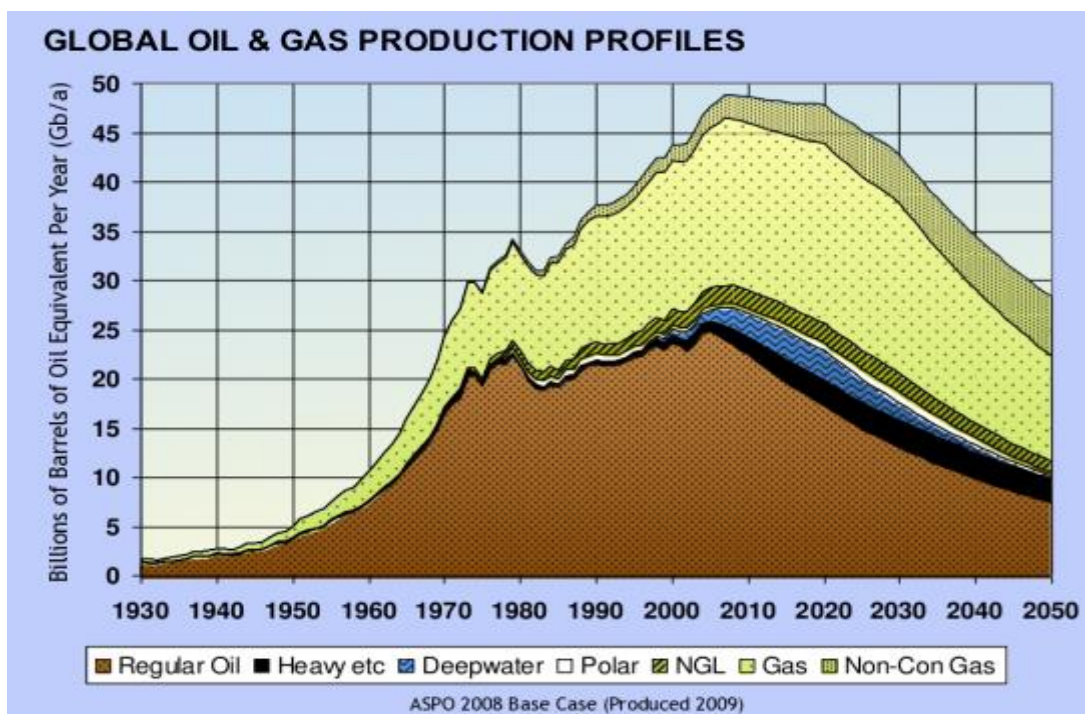


Fig. 2 Realistic model of oil and gas production (1)

In the North Sea sector EOR methods have taken place since 1974. The methods are involved in mature oil fields from the moment that production starts to decrease. Thus, the field can achieve a second peak of production.

# 1. Enhanced Oil Recovery (EOR)

The hierarchy of oil production includes primary recovery, secondary recovery and tertiary recovery. Tertiary recovery is preceded by secondary and primary recovery. (Fig.3)

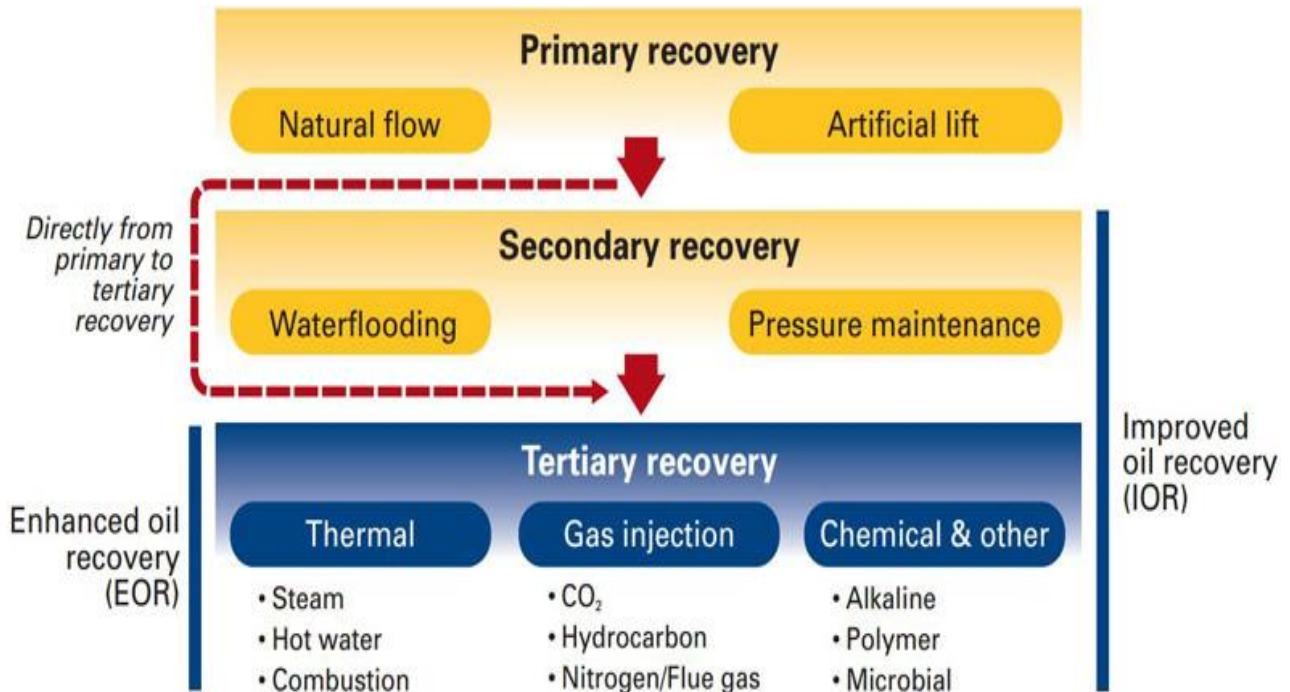


Fig. 3 Hierarchy of oil production <sup>(2)</sup>

On Fig.3 is depicted the hierarchy of oil production. Also it suggests that some parts of it can be avoided based on the reservoir characteristics. For example if the reservoir does not have sufficient energy for developing primary recovery then secondary recovery has to be applied from day one of production. Also in some cases secondary recovery can be skipped. In those cases secondary methods will not be sufficient to improve the recovery.

Primary recovery is a result from forces naturally accruing in the reservoir. Those forces reflect the natural energy which exists in the reservoir and supports the production of hydrocarbons. Sources of natural energy are: solution gas drive; gas cap drive; natural water drive; fluid and rock expansion; gravity drainage. Secondary recovery is implemented after primary recovery in order to support the decreasing pressure in the reservoir and simultaneously to increase the production. It includes waterflooding and maintenance of the pressure. Gas injections also can be included as a secondary recovery method only if the gas is immiscibly injected to displace the oil. In that case the gas does not change characteristics neither of the reservoir nor of the fluids. Combined primary and secondary recovery processes might recover up to 40% of original oil in place (OOIP). This is around 1/3 of the OOIP in the reservoir which is a relatively low percent. Ranges for the primary and secondary recovery can be different based on oil type.

Oil Type	Primary Recovery % of OOIP	Secondary Recovery % Extra of OOIP
Extra Heavy	1 – 5	–
Heavy	1 – 10	5 – 10
Medium	5 – 30	5 – 15
Light	10 – 40	10 – 25

From Shell

Fig. 4 Percentage of OOIP extracted through primary and secondary recovery

Low recovery values can be related with unfavorable reservoirs (high heterogeneous rocks; less permeable), high oil viscosity and less solution gas drive.

EOR methods (part of the tertiary recovery) are applied after secondary recovery. “Enhanced oil recovery (EOR) is oil recovery by the injection of materials not normally present in the reservoir (L. W. Lake)”.

It is focused mainly on heavy oil extraction but it is also applied on medium and light oil. Aim of the EOR methods is to increase the recovery factor which reflects the amount of extracted oil. EOR methods are aiming in decreasing residual oil saturation - oil fraction which is left behind after primary and secondary recovery and cannot be extracted by ordinary fluid drives and recovery techniques. Recovery factor is the ratio between amount of the extracted oil and the amount of oil which is originally contained in the reservoir (3). It is numerically presented in fractions of a unit or in percentage.

$$\text{Recovery factor} = \frac{\text{Estimate of recoverable oil}}{\text{Estimate of in place oil}} \quad (1)$$

Changes in the recovery factor with time are reflection of the applied methods for enhancing the recovery. EOR encompass methods for improving the oil production and increasing the recovery factor.

Estimation of fluid saturation in reservoir is mandatory in order to identify gas, oil and water zones in the reservoir. Based on that can be calculated the initial oil or gas saturation in place and the zones, where the left behind oil is focused. This is included in evaluation of the EOR processes.

Regarding the individual saturation of the particular fluid (oil, gas, water) in the porous media can be estimated the relative amount of fluids which flow in the reservoir. Due to the production, in the reservoir can occur a new phase (for ex. free gas). This can result in additional recovery.

Fluid saturation is presented in percent or as a fraction of pore space. In reservoirs with absence of gas sum of oil and water saturation adds up to unity (100%) of the pore space. (4)

$$S_{oi} + S_{wi} = 1 \quad (2)$$

Where:

$S_{oi}$  – initial oil saturation;

$S_{wi}$  – initial water saturation;

Saturation of oil and water changes with time and location. This controls relative flow of fluid (oil, water) towards the wellbore. Due to the high specific gravity of water, its saturation increases with reservoir depth. Specific gravity is the ratio of the density of the substance (oil) to the density of a reference substance (water) for mass of the same unit volume. (5)

$$\gamma_o = \frac{\rho_o}{\rho_w} \quad (3)$$

Where:

$\gamma_o$  – specific gravity of the oil – unitless;

$\rho_o$  – density of the crude oil –  $\text{kg/m}^3$ ;

$\rho_w$  – density of the water –  $\text{kg/m}^3$ .

Initial hydrocarbon saturation which can be exhibited in a producing reservoir excess 70% of pore space. The other 30% are filled with formation water and referred as connate water saturation. Connate water saturation is formed during the deposition of the rock.

Initial oil formation volume factor (FVF) refers to the volume changes in oil as a result due to change into conditions (from reservoir to surface) regarding pressure reduction. FVF is the ratio of reservoir barrels over stock-tank barrels (rb/stb) and can be defined as follow: (4)

$$B_o = \frac{\text{Volume of oil + dissolved volatiles: both under reservoir pressure and temperature}}{\text{Volume of produced oil under stock tank conditions following gas liberation}} \quad (4)$$

Where:

$B_o$  – oil formation volume factor – rb/stb.

Concept of EOR is based on the fact that there is a considerably high amount of oil left in the reservoir after primary and secondary recovery. Objective of the EOR methods is to mobilize the residual oil throughout the volume of the reservoir. This is achieved by improving oil displacement and volumetric sweep efficiency.

Displacement efficiency encompasses *microscopic* and *macroscopic* displacement efficiency (4). Microscopic displacement efficiency characterizes the displacement of oil by displacing fluid on the pore scale level. It measures how well the displacing fluid mobilizes the residual oil. Poor microscopic displacement efficiency is due to the capillary forces which are the main force controlling fluid distribution on pore level. Macroscopic displacement efficiency is concerned with fluids in contacting the reservoir in a volumetric sense. It measures how effectively the displacing fluid sweep out the volume of the reservoir in both directions – areally and vertically.

$$E_V = E_{VS} \cdot E_{AS} \quad (5)$$

Where:

$E_V$  – microscopic displacement efficiency;

$E_{VS}$  – vertical microscopic displacement efficiency;

$E_{AS}$  – areal microscopic displacement efficiency.

Volumetric sweep efficiency is the ratio between the volume of oil contacted by the displacing fluid and the volume of oil originally in place (Lake, 1989). The equation for calculating the volumetric sweep efficiency uses the relation between oil recovery factor and displacement efficiency. (4)

$$E_R = E_{displ} \cdot E_{vertical} \cdot E_{areal} \quad (6)$$

If

$$E_{vol} = E_{vertical} \cdot E_{areal} \quad (7)$$

Therefore,

$$E_{vol} = \frac{E_R}{E_{displ}} \quad (8)$$

Where:

$E_{vol}$  – volumetric sweep efficiency;

$E_R$  – recovery factor;

$E_{displ.}$  – displacement efficiency.

Important characteristic is wettability of the reservoir rock. This is the tendency of one immiscible fluid (oil or water) to adhere to the pore walls. Wetting fluid is the fluid with higher affinity to the solid surface and it fills preferentially the narrowest parts of the pore space. Nonwetting fluid occupies the largest parts of pore space.

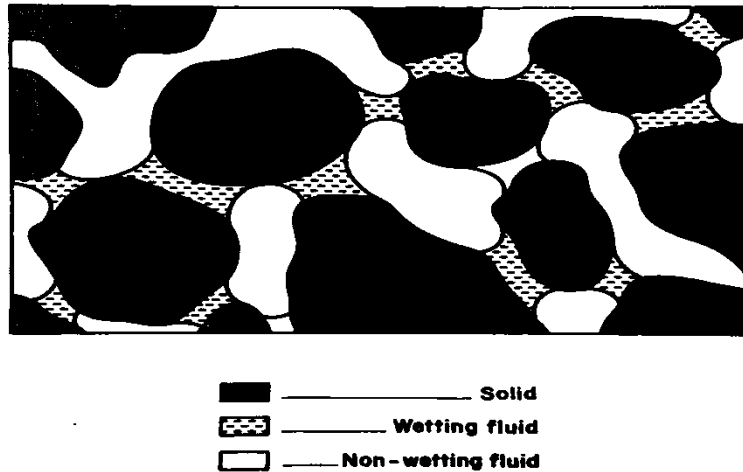


Fig. 5 Distribution of two immiscible fluids at pore scale (6)

If the oil pressure is higher than water pressure oil droplets cannot pass through the narrowest part of the channel's width. In Nagani oil field is assumed that wetting fluid is water and nonwetting is oil. This is based on the fact that relative permeability of the nonwetting fluid is higher than the relative permeability of the wetting fluid. Nonwetting fluid flows easily because it occupies the largest pores.

Table 1 Values for water saturation ( $S_w$ ) and residual water and oil permeability ( $K_{wr}$  and  $K_{or}$ ) – Nagani oil field Eclipse data file

$S_w$	$K_{wr}$	$K_{or}$
0.2	0	0.9
0.22	0	0.813
0.2925	0.0002	0.5446
0.365	0.0031	0.343
0.4375	0.0158	0.1985
0.51	0.05	0.1016
0.5825	0.1221	0.0429
0.6	0.15372	0.03561
0.655	0.2531	0.0127
0.7275	0.4689	0.0016
0.8	0.8	0
1	1	0

On Table 1 are introduced the values for  $S_w$ ,  $K_{wr}$  and  $K_{or}$  implemented in Eclipse simulation data file for Nagani oil field.

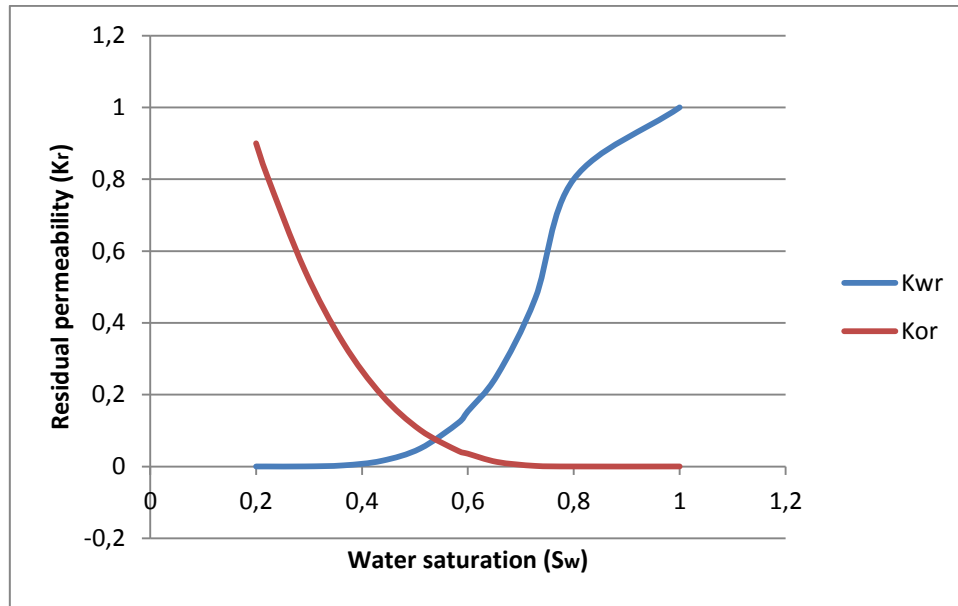


Fig. 6 Relative Permeability as a function of wetting fluid saturation for Nagani oil field

Fig.6 is depicts the plot of relative permeability ( $K_r$ ) as a function of water saturation ( $S_w$ ). It is assumed that water is the wetting and oil is the nonwetting fluid in the system. The plot is constrained based on the information received from Table 1.

At reservoir scale the capillary forces do not have an important overall effect on the fluid distribution. Important effects have gravity forces and pressure distribution (regarding location of injector and production wells, and local properties of the reservoir).

Capillary forces have an important effect on displacing oil with immiscible fluid if the reservoir is heterogeneous. Capillary forces tend to drive the oil from the low permeability layers to high permeability layers and vice versa for the water in order to equalize the capillary pressure in both layers.

Displacement of oil in the reservoir by displacing fluid results in formation of transition zone between the oil and displacing fluid. This transition zone increases with the time. To achieve higher production it is necessary to decreased thickness of the transition zone, when the displacing fluid reaches the production well. Oil displacing fluids can be immiscible, partially miscible or miscible.

#### Oil displacement by immiscible fluid:

During the oil displacement by immiscible fluid, oil is pushed throughout the pore space based on the pressure difference between two sides of the interface - *Laplace formula* (6):

$$P_o - P_w = \sigma c \quad (9)$$

Where:

$P_o$  – pressure of the oil;

$P_w$  – pressure of the water;

$\sigma$  – interfacial tension of the oil-water interface;

$c$  – mean curvature of the oil droplet.

This equation is applied mainly for fluids in rest but it remains approximately valid when the fluids are flowing as a result from the fact that the capillary forces are much bigger than viscosity forces.

When the displacing fluid reach the production well it does not mean that the whole reservoir has been swept. There is a possibility that there have been some parts of the reservoir which were bypassed and still contain most of the initial oil. Due to the displacement process a transition zone is formed.

#### Oil displacement by partially miscible fluid:

The mechanism of displacement by partially miscible fluid is similar to the previous one. The difference is that part of the fluid reacts with the oil by exchanging elements. Based on that is formed a mixing zone. In this zone fluid composition varies continuously between the composition of oil and the composition of the displacing fluid. As a result oil displacement process is more efficient.

#### Oil displacement by miscible fluid:

This mechanism is the most efficient because the displacing fluid exchanges components with the oil until it becomes a single fluid phase with varying composition. By exchanging components it transports the oil throughout the porous space. Velocity of the flow is faster in the large sections of the pores. If there is a bypassed zone in the reservoir it still can be swept - as a result from diffusion process oil is transferred from bypassed zone to the zones with higher flow velocity. Due to the continuous production this oil can be recovered regarding the fact that it is not completely trapped.

Transition zone which is formed due to the displacement by immiscible displacing fluid is thicker than the one formed by partially miscible displacing fluid. To decrease the thickness of transition zone and corresponding oil saturation is needed to decrease the mobility ratio.

Proportion of the unswept areas depends on the mobility ratio (6):

$$M = \frac{\lambda_d}{\lambda_o} = \frac{K_d \mu_o}{K_o \mu_d} \quad (10)$$

Where:

$\mu_o$  – oil viscosity - cp;

$\mu_d$  – displacing fluid viscosity - cp;

$K_o$  – effective oil permeability;

$K_d$  – effective displacement fluid permeability;

$$\lambda_o = \frac{K_o}{\mu_o} - \text{mobility of the oil};$$

$$\lambda_d = \frac{K_d}{\mu_d} - \text{mobility of the displacing fluid.}$$

The mobility ratio reflects the difference in the mobility between the displacing and the displaced fluids (water and oil). Based on the received value due to the calculation M is assigned to be favorable or unfavorable. To be assessed as favorable the mobility ratio needs to gain value between 0 and 1. Therefore, the mobility ratio is evaluated as unfavorable gives a value higher than 1. Improvement in the mobility ratio results in improvement in displacement efficiency.

If the displacement fluid is more mobile than displaced fluid there is a high possibility to occur viscous “fingering” in homogeneous porous media. This will lead to poor sweep efficiency in recovery method. When the viscosity of the displacing fluid is lower than viscosity of the displaced fluid – gas and oil, measures are taken to avoid viscous fingering. Rearranging the location of production and injection wells in a manner that gravity forces will tend to reduce the growth rate of the fingers is a reasonable solution. In this case the displacement will occur downwards. It can be assumed also that the viscous fingering is eliminated when the flow rate is lower than some critical value. The critical value expressed as a Darcy velocity is introduced by the following equation (6):

$$u_c = \frac{k(\rho_o - \rho_d)g \sin \alpha}{\left(\frac{\mu_o}{K_{or}}\right) - \left(\frac{\mu_d}{K_{dr}}\right)} \quad (11)$$

Where:

k – permeability;

g – gravity acceleration;

$\alpha$  – the dip-angle of the layer;

$\rho_o$  – oil density;

$\rho_d$  – density of the displacing fluid;

$K_{or}$  – relative permeability to oil in oil zone;

$K_{dr}$  – relative permeability to displacing fluid in the swept zone.

## 1.1 Screening criteria for EOR methods

There are many variables which should be considered in order to design an EOR process for particular reservoir. Those variables include: oil type, reservoir rock, reservoir depth, formation type, oil saturation and past production methods. Because of the different reservoir parameters it is impossible to be developed and applied a single universal methodology to every reservoir. Screening is the first step for implementing an EOR method. Due to the screening different reservoir parameters have to be evaluated. Based on this evaluation for a reservoir can be selected several methods from which by more detailed study one of them is chosen.

Screening criteria are based on oil and reservoir properties. Those criteria encompass ratios of parameters received from field and laboratory operations. A convenient screening criteria is API gravity.

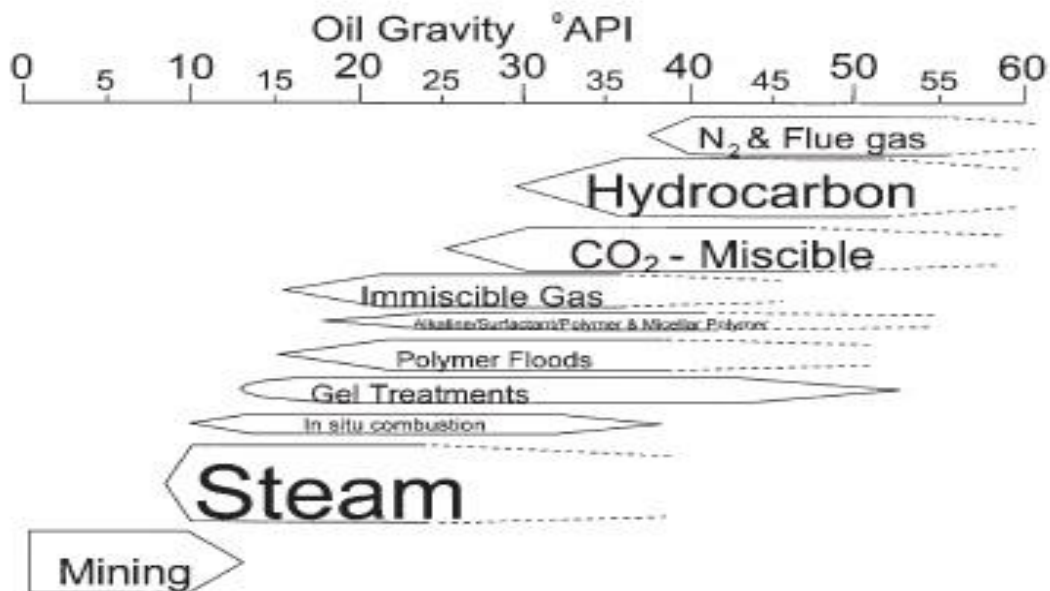


Fig. 7 Screening for EOR method based on API gravity <sup>(7)</sup>

On the Fig. 7 are depicted the approximated ranges of oil gravity for each of the EOR methods. The size of the type on the figure reflects the importance of each EOR method in terms of current incremental oil production.

Choice of the EOR method for the particular case is based on the screening criteria. Screening criteria suggested by J. J. Taber (1997) <sup>(7)</sup> are based on successful EOR projects and improved through the years understanding of required conditions for the different EOR methods. Provided screening criteria are covering eight EOR methods which has been evaluated as the most important.

Table 2 Summary of screening criteria for EOR methods <sup>(7)</sup>

Detail Table in Ref. 16	EOR Method	Oil Properties			Reservoir Characteristics					
		Gravity (°API)	Viscosity (cp)	Composition	Oil Saturation (% PV)	Formation Type	Net Thickness (ft)	Average Permeability (md)	Depth (ft)	Temperature (°F)
Gas Injection Methods (Miscible)										
1	Nitrogen and flue gas	>35, <u>48</u> <sup>a</sup>	<0.4, <u>0.2</u> <sup>a</sup>	High percent of C <sub>1</sub> to C <sub>7</sub>	>40, <u>75</u> <sup>a</sup>	Sandstone or carbonate	Thin unless dipping	NC	> 6,000	NC
2	Hydrocarbon	>23, <u>41</u> <sup>a</sup>	<3, <u>0.5</u> <sup>a</sup>	High percent of C <sub>2</sub> to C <sub>7</sub>	>30, <u>80</u> <sup>a</sup>	Sandstone or carbonate	Thin unless dipping	NC	> 4,000	NC
3	CO <sub>2</sub>	>22, <u>36</u> <sup>a</sup>	<10, <u>1.5</u> <sup>a</sup>	High percent of C <sub>5</sub> to C <sub>12</sub>	>20, <u>55</u> <sup>a</sup>	Sandstone or carbonate	Wide range	NC	>2,500 <sup>a</sup>	NC
1-3	Immiscible gases	> 12	<600	NC	>35, <u>70</u> <sup>a</sup>	NC	NC if dipping and/or good vertical permeability	NC	> 1,800	NC
(Enhanced) Waterflooding										
4	Micellar/Polymer, ASP, and Alkaline Flooding	>20, <u>35</u> <sup>a</sup>	<35, <u>13</u> <sup>a</sup>	Light, intermediate, some organic acids for alkaline floods	>35, <u>53</u> <sup>a</sup>	Sandstone preferred	NC	> 10, <u>450</u> <sup>a</sup>	> 9,000, <u>3,250</u>	>200, <u>80</u>
5	Polymer Flooding	> 15	<150, >10	NC	>50, <u>80</u> <sup>a</sup>	Sandstone preferred	NC	>10, <u>800</u> <sup>a, b</sup>	< 9,000	>200, <u>140</u>
Thermal/Mechanical										
6	Combustion	> 10, <u>16</u> →?	< 5,000 ↓ <u>1,200</u>	Some asphaltic components	>50, <u>72</u> <sup>a</sup>	High-porosity sand/sandstone	>10	> 50 <sup>c</sup>	<11,500, <u>3,500</u>	>100, <u>135</u>
7	Steam	> 8 to <u>13.5</u> →?	<200,000 ↓ <u>4,700</u>	NC	>40, <u>66</u> <sup>a</sup>	High-porosity sand/sandstone	>20	>200, <u>2,540</u> <sup>a, d</sup>	<4,500, <u>1,500</u>	NC
—	Surface mining	7 to 11	Zero cold flow	NC	>8 wt% sand	Mineable tar sand	> 10 <sup>e</sup>	NC	> 3:1 overburden to sand ratio	NC
NC = not critical. Underlined values represent the approximate mean or average for current field projects. <sup>a</sup> See Table 3 of Ref. 16. <sup>b</sup> > 3md from some carbonate reservoirs if the intent is to sweep only the fracture system. <sup>c</sup> Transmissibility > 20 md-ft/cp <sup>d</sup> Transmissibility > 50 md-ft/cp <sup>e</sup> See depth.										

All of the values introduced in Table 2 are varying in a different interval. Even if some of the reservoir characteristics to deviate from those given in the particular case it is still possible to be achieved positive results by implementing the method.

## 1.2 EOR methods

EOR methods include recovery processes only inside the reservoir. Their purpose is to recover as much as possible incremental oil.

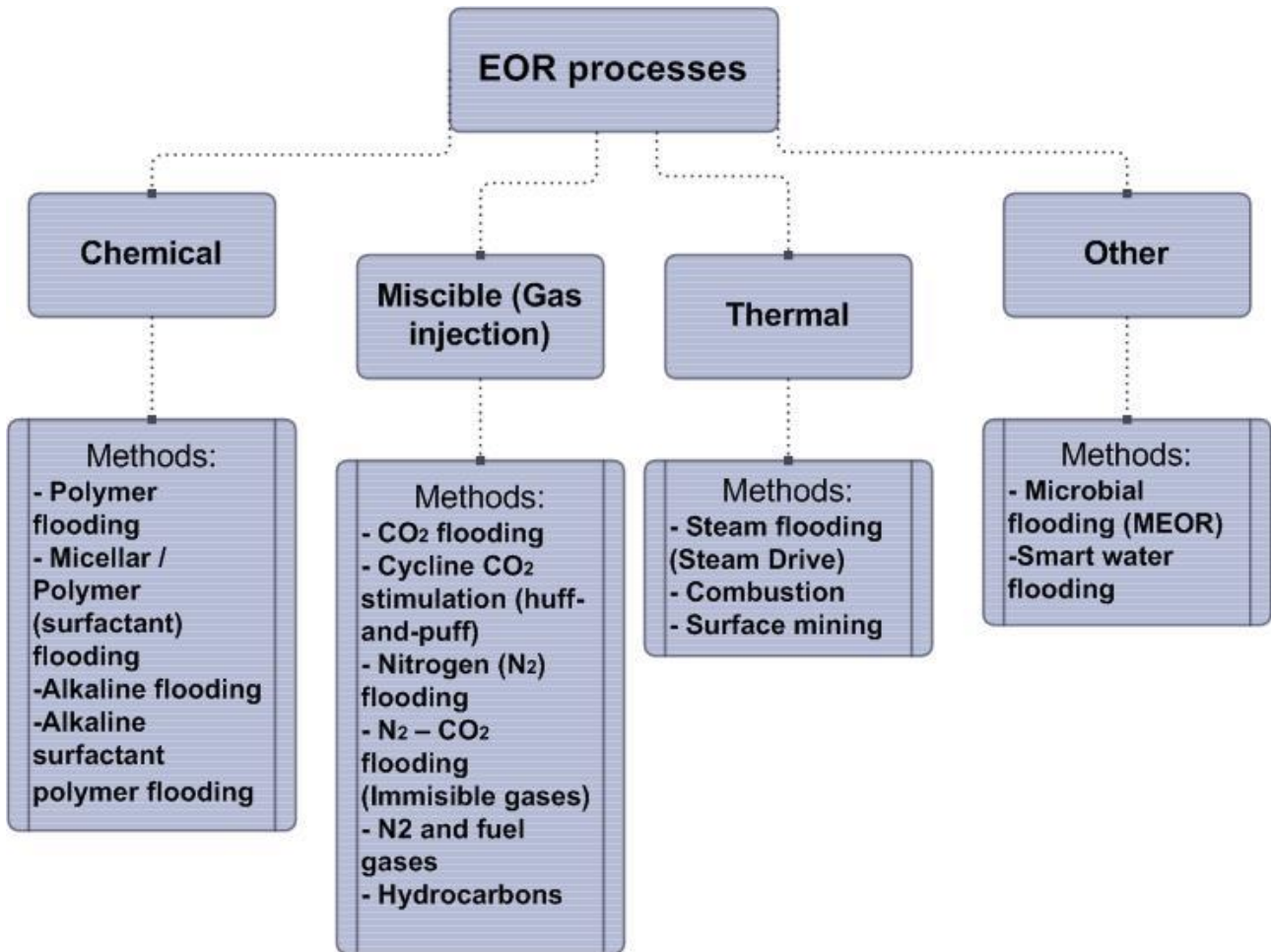


Fig. 8 EOR processes - classification and methods

Each group of methods is applicable for specific range of oil and reservoir characteristics.

Gas flooding methods are becoming more and more extensively used since their implementation is economically efficient. Surfactant flooding is still developing and requires more research and experiments for mastering the process and also improving the used products and decreasing the operating costs.

Implementation of EOR methods is preceded of detail evaluation of the reservoir characteristics. Due to this evaluation are summarized the main oil properties and reservoir characteristics.

On the figure below are illustrated the factors upon which the different kinds of EOR methods act.

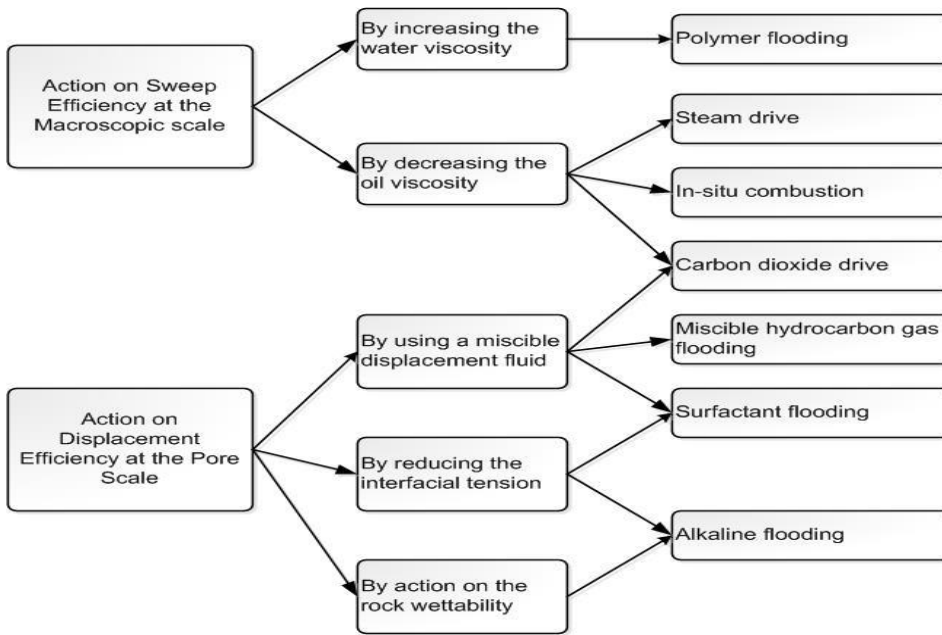


Fig. 9 Factors upon which the main types of enhanced oil recovery methods act (6)

As a result of decreasing oil production the urge of selecting the best EOR method for the particular field has increased.

### 1.3 Selection of EOR method

Selection of the EOR methods in this project's case is made according to the following oil properties and reservoir characteristics:

- API gravity
- Viscosity
- Oil saturation
- Formation type and net thickness of reservoir
- Reservoir depth

API gravity is used to compare the relative density of petroleum liquids. It measures how light or heavy the crude oil is. High API gravity suggests lighter composition of the oil. For calculating API gravity is needed the specific gravity (SG) of the oil<sup>(5)</sup>. It is calculated by applying the equation for calculating SG (3):

$$\gamma_o = \frac{\rho_o}{\rho_w} = \frac{875.3}{1020.3} = 0.858 \text{ kg/m}^3$$

Specific gravity of the oil is estimated to be equal to 0,858 kg/m<sup>3</sup>. Estimation is reasonable because of the relation between viscosity and density of the oil.

API gravity is calculated through the SG of the oil by applying the following equation <sup>(5)</sup>:

$$API = \frac{141.5}{\gamma_o} - 131.5 \quad (12)$$

$$API = 33.4$$

According to the measured value for API gravity oil can be classified as light, medium, heavy or extra heavy. Value of the API<sup>o</sup> received for the dead oil produced from Nagani oil field corresponds to the range for light to medium oil.

Oil type:	API gravity
Light oil	>31.1 (less than 870 kg/m <sup>3</sup> )
Medium oil	22.3 < API <sup>o</sup> <31.1 (870 to 920 kg/m <sup>3</sup> )
Heavy oil	<22.30 (920 to 1000 kg/m <sup>3</sup> )
Extra heavy oil	<10.0 (greater than 1000 kg/m <sup>3</sup> )

Table 3 Classification of the crude oil according to its API gravity (8)

Viscosity along with the AIP gravity is a main parameter for selection of EOR method. In order to calculate the viscosity of the oil is needed the reservoir temperature. Calculation of the reservoir temperature is based on the temperature gradient. Geothermal gradient is the rate with which the temperature is increasing with increasing depth in the Earth`s interior. Value of geothermal gradient used for calculating the reservoir temperature is assumed to be 25<sup>o</sup>C/km (77<sup>o</sup>F/km). Due to the accuracy of the temperature value received for the reservoir it is needed to be added the ambient (surface) temperature. For onshore conditions it is 20<sup>o</sup>C and for offshore conditions it is 10<sup>o</sup>C.

Basically reservoir temperature is a direct function of the reservoir depth and it is calculated by the following equation <sup>(9)</sup>:

$$T_r = T_s + (Temperature\ gradient * D) \quad (13)$$

WhEre:

T<sub>r</sub>– reservoir temperature;

T<sub>s</sub> – ambient (surface) temperature;

D – reservoir depth.

Calculating of the dead oil viscosity is done by applying the equation suggested by H. D. Beggs (1975)<sup>(10)</sup>:

$$\mu_{OD} = 10^x - 1 \quad (14)$$

Where

$$x = y * T^{-1.163}$$

$$y = 10^z$$

$$z = 3.0324 - 0.02023 * \gamma_o$$

Where:

$\mu_{OD}$  – dead oil viscosity - cp;

T – reservoir temperature -<sup>o</sup>F ;

Results received from calculating the temperature and dead oil viscosity are depicted on the table below:

**Table 4 Results from temperature and viscosity calculations**

	<b>with ambient t =20<sup>o</sup>C</b>	<b>with ambient t =10<sup>o</sup>C</b>
<b>Temperature in <sup>o</sup>C</b>	70.5	60.5
<b>Temperature in <sup>o</sup>F</b>	158.9	140.9
<b>x</b>	0.61	0.70
<b><math>\mu_{od}</math> (cp)</b>	<b>3</b>	<b>4</b>

Location of the Nagani oil field is unknown. Because of that on Table 4 are illustrated the difference in the results from calculations based on the location (onshore or offshore). For further calculations in this case will be used the viscosity value of 4 evaluated based on temperature equation (13) including the temperature gradient corresponding to offshore conditions.

In order to ensure the accuracy of the applied equations for calculating the viscosity was conducted a laboratory experiment (Appendix A). Due to the experiment was observed the change in the viscosity of dead oil with increasing the temperature.

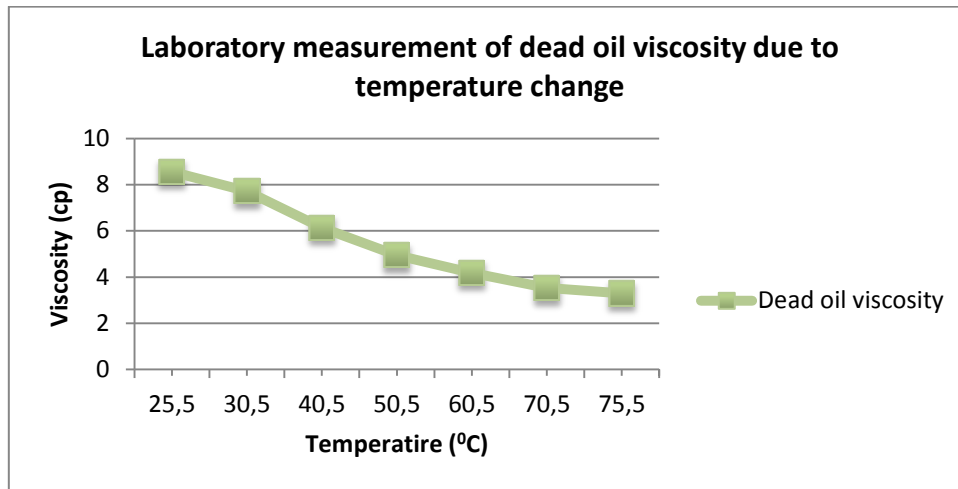


Fig. 10 Laboratory measurements of the dead oil viscosity

Table 5 Depiction of the viscosity values regarding the change in the temperature

Temperatur (°C)	Viscosity (cp)
<b>25.5</b>	<b>8.56</b>
<b>30.5</b>	<b>7.72</b>
40.5	<b>6.13</b>
50.5	<b>4.95</b>
<b>60.5</b>	<b>4.18</b>
70.5	<b>3.53</b>
75.5	<b>3.3</b>

Fig.10 and Table 5 depict the change in the viscosity of the dead oil with increasing temperature. The viscosity value received experimentally for the estimated temperature for Nagani oil field corresponds to the calculated viscosity value (14).

Received value for the viscosity of the oil makes possible application of equation (10) for assessing the mobility ration between the water and the oil. For calculation of the mobility ratio was used end points relative permeability data.

$$M = \frac{k_{wr}\mu_o}{k_{or}\mu_w} = \frac{1 * 4}{0.9 * 0.4} = 11$$

Based on the received value can be concluded that the mobility ratio is clearly unfavorable. Therefore the improvement is necessary.

Saturation is an important parameter which characterizes the relative amount of oil, water and gas in the reservoir. Based on the relative oil saturation is estimated the profitability of further implementation of EOR methods. Oil saturation is required to be higher than 35% for implementing EOR. Oil saturation in the beginning of production is estimated by an original oil-in-place volumetric equation (11):

$$OOIP = \text{Rock Volume} * \phi * (1 - S_{wr}) * \frac{1}{B_o} \quad (15)$$

Where:

OOIP – original oil-in-place;

$\phi$  - Porosity;

$S_{wr}$  – Residual water saturation;

$B_o$  – Formation volume factor of oil.

Pore rock volume of the reservoir is equal to 1 586 699 759 m<sup>3</sup>. Formation volume factor for oil is assumed to be equal to 1 because there is no information for gas production during the years from Nagani oil field. It can be concluded, that there is no significant volume changes in the oil, from reservoir to surface conditions regarding pressure reduction.

Originally in the reservoir OOIP = 53 042 824 m<sup>3</sup> / 333 629 325.7 STB. By applying equation (15) is received the value for  $S_w = 0.20$ , from where by applying the relation  $S_o = 1 - S_w$  follows that  $S_o = 0.80$ . Those saturation values reflect the initial saturation in the beginning of production.

Current OOIP after six years of production (day 2238) by waterflooding technique is equal to 39 694 692 m<sup>3</sup> / 249 672 095 STB. From it can be calculated the residual oil saturation.

Displacement efficiency is a parameter which reflects the amount of movable oil which has been produces (displaced) from the swept zone as a fraction of the initial total oil volume in the reservoir<sup>(12)</sup>.

$$E_D = \frac{\text{Volume of the oil at start of flood} - \text{Remaining oil volume}}{\text{Volume of the oil at start of flood}} \quad (16)$$

$$E_D = \frac{53\,042\,824 - 39\,694\,691}{53\,042\,824} = 0.25$$

Where:

$E_D$  – displacement efficiency;

Received value for displacement efficiency is used for calculating the average oil saturation in the swept zone due to the water flooding<sup>(12)</sup>.

$$E_D = \frac{\frac{S_{oi}}{B_{oi}} - \overline{S_o}}{\frac{S_{oi}}{B_{oi}}} \quad (17)$$

Where:

$S_{oi}$  – initial oil saturation at the start of flood;

$B_{oi}$  – oil FVF at start of flood;

$\overline{S_o}$  - average oil saturation at the flood pattern.

Based on the fact that there is no gas produced throughout the production period of the field it can be said that  $FVF=1=\text{constant}$ . In this case it is excluded from the equation.

$$E_D = \frac{S_{oi} - \overline{S_o}}{S_{oi}} \quad (18)$$

From where,

$$\overline{S_o} = 0.6$$

Average oil saturation is also given by:

$$\overline{S_o} = 1 - \overline{S_w}$$

The average water saturation in the swept area ( $\overline{S_w}$ ) is calculated to be equal to 0.4.

Average oil saturation of the swept area due to the production period refers to the residual oil saturation.

All of the parameters used for screening for EOR method are summarized below (Table 6):

Table 6 Reservoir screening parameters

Parameters:	
API <sup>o</sup> gravity	33.4
Viscosity	4 cp
Residual oil saturation	60 (%)
Formation type	sandstone
Net thickness of reservoir	229.6 ft
Reservoir depth	6 627.3 ft

Selection of an EOR method applicable to this reservoir was made based on the EOR screening criteria by Taber (1997)<sup>(7)</sup>. Those criteria for the different EOR methods are presented on table 2.

Unselected methods are not appropriate for the particular case which makes their implementation inefficient for the particular reservoir.

**Thermal methods** are not acceptable because their main target is heavy to extra heavy oil or tar sands. For application of thermal methods are required also high viscosity, high vertical permeability and small reservoir depth.

**Miscible (Gas injection) methods** are not appropriate for the particular case because they are mostly implemented in carbonate reservoirs. Also their main targets are light, condensate and volatile oil reservoirs with specific oil composition and very low viscosity value.

**Chemical methods** are most likely to be appropriate for the particular case because they require conditions which are favorable to water injection. This is because they can be accepted as a modification of waterflooding. Micellar - polymer flooding, Alkaline flooding and Alkaline-surfactant-polymer flooding are not appropriate because they require specific oil composition, gas presence, oil as a wetting fluid.

Based on table 2 was selected Polymer flooding method. This method can be referred also as a mobility control method.

Reservoir parameters correspond to a large extent the criteria for applying the Polymer flooding method. Despite the disparity in viscosity value with the range of viscosity values introduced for the polymer flooding it was selected regarding the other available oil and reservoir characteristics.

### 1.3.1 Polymer flooding

Polymer flooding is one of the chemical EOR methods which have major importance today. It is focused on reducing the mobility ratio by involving an addition of polymers into the injected water. Due to the polymer flood a long chain molecules called polymers are added to the injected water. Polymer acts by increasing the viscosity of the water which improves the mobility ratio and increases the recovery efficiency. Polymers can increase water viscosity between 3 and 20 times even at very low concentration of a few hundreds of

ppm (parts per million). The increased viscosity of the water provides more stable oil displacement. (Fig.10)

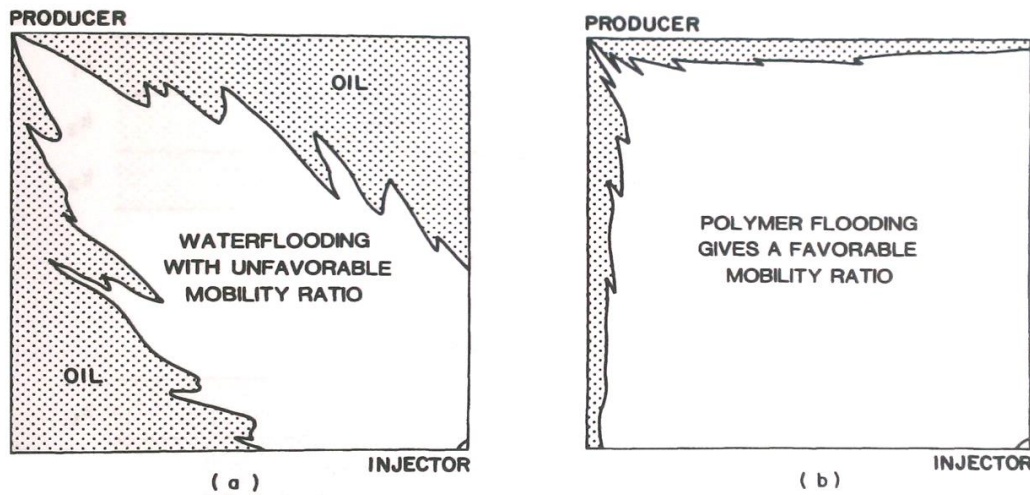


Fig. 11 Improvement in areal sweep efficiency by use of polymer – (a) unfavorable mobility ratio; (b) favorable mobility ratio; (6)

Fig.11 illustrates the improvement of the mobility ratio as a result from added polymers (b) compared with ordinary water flooding (a). Presence of polymers in the displacing phase decreases the mobility ratio by increasing the viscosity of the water. This provides more stable front of displacement and avoids occurring of large scale fingering or channeling.

In a solution polymers exhibit the behavior of a non-Newtonian fluid. Non-Newtonian are the fluids which behavior defers from the behavior of Newtonian fluids. Their demeanor is dependent on the shear rate. The non-Newtonian fluids have a non-linear relation between shear rate and shear stress. Because of that they can exhibit different types of non-Newtonian behavior. The viscosity of the polymer solution is called apparent viscosity. Apparent viscosity is a term used to describe the viscosity of a non-Newtonian fluid, measured with methods applied for Newtonian fluids. In order to be observed the change of the brine viscosity by adding polymers, have been conducted a series of experiments. The objective of the experiment was to create a polymer solution with viscosity close to the viscosity of the crude oil introduced in this project and observed the changes due to increase in the temperature. For that purpose were prepared two brine solution – 40 g/l salt and 60 g/l salt, in order to illustrate also effect of the salinity on the change into viscosity. For the experiments were used two types of the polymer polyacrylamide (PAM - P 70-65 and PAM - P 70-50), received from water treatment plant (Bo Jensen Vandbehandling A/S). In total were prepared 38 samples with varying amount of polymer dissolved in 50ml brine solution. Due to the experiment was observed that the rate with which the viscosity of the polymer solution increases is relatively higher for the higher salinity solution (Appendix A). As result from the experiment was prepared a polymer solution with viscosity corresponding to the oil viscosity. Also it was observed that it exhibits shear thickening. (Appendix A)

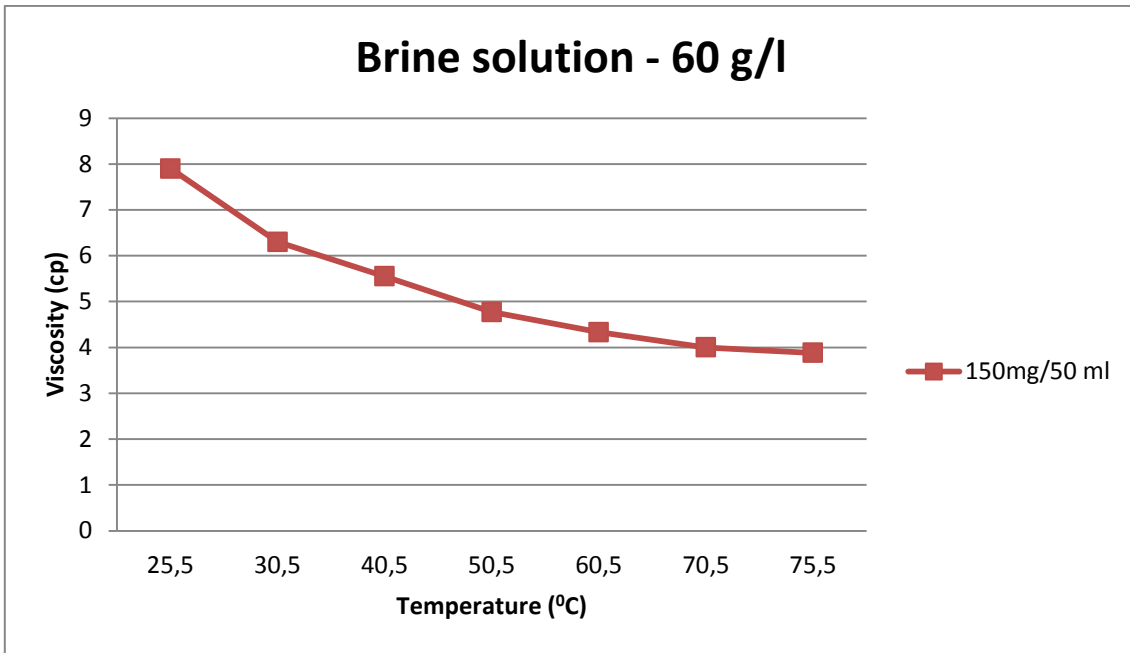


Fig. 12 Change into viscosity for the polymer sample with apparent viscosity closer to the oil's

Moreover, decreasing rock formation permeability by polymers in heterogeneous reservoirs is of paramount importance. Decreasing the permeability in more porous localities (layers) of the reservoir concludes in enhancing the displacement from less porous/permeable layers.

Application of the polymer flooding provides oil extraction from low-permeable regions, which initially were bypassed due to water flooding. Most likely those regions contain amounts of oil higher than the residual oil saturation.

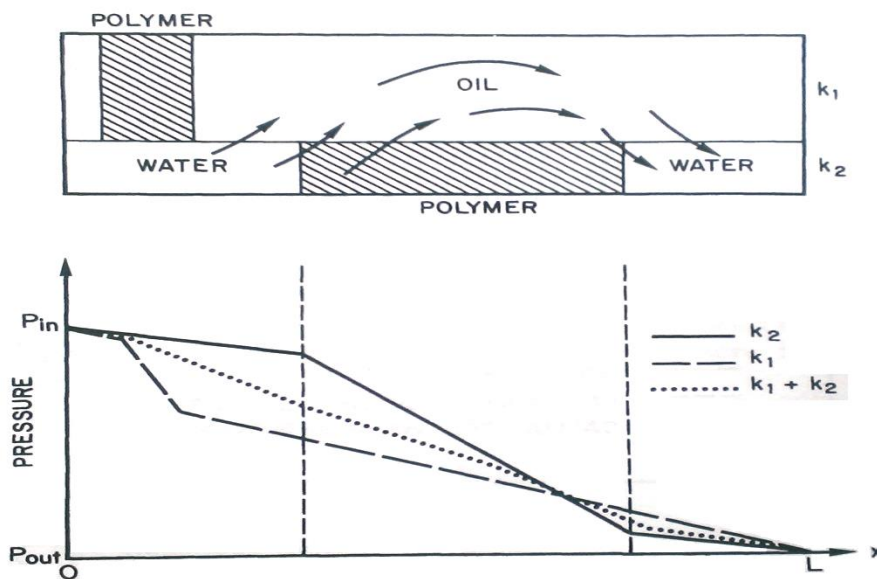


Fig. 13 Crossflow effect in polymer flood of layered reservoir<sup>(6)</sup>

Fig. 13 introduces the crossflow effect of the polymer flood in layered reservoir with different values for permeability ( $k_1 > k_2$ ). Due to the plugging effect of the polymer slug in the high permeable layer chase water at the rear which carries a little amount of polymers, is derived out in the low permeable layer. Displaced oil from the low permeable layer is driven by the water to a high permeable layer. Due to the flow of chase water the polymer slug in the high permeable layer will be lost. This process acts in the neighborhood of the slug. That is the reason why the oil displaced from the low permeable layer is produced from the high permeable layer.

Two main types of polymers (macromolecules) are used in the process of polymer flooding – partially hydrolyzed polyacrylamide (HPAM) and xanthan. Xanthan is a biopolymer which reduces the mobility ratio by increasing the solution viscosity. HPAM improves the unfavorable mobility ratio as a result from increased solution viscosity and decreased rock permeability due to the polymer retention.

There are three mechanisms of polymer retention with different locations illustrated on Fig. 14. Such include:

- Hydrodynamic retention;
- Adsorption on the pore surface;
- Mechanical entrapment.

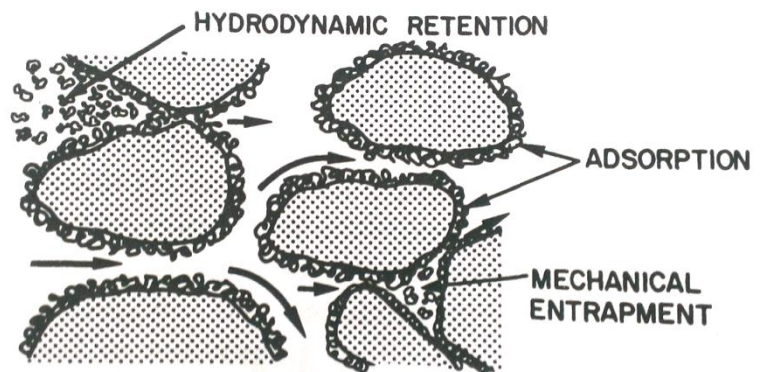


Fig. 14 Location of the main types of polymer retention in the porous media flow <sup>(6)</sup>

*Hydrodynamic retention* introduces the local accumulation of polymer molecules as a result from diffusion- convection controlled mechanism. During low flow rates, a positive linear correlation can be found between the retention of the polymer and the amplification/increment of the flow rate, with consequent decrease based on the molecule size diminution derived from the concentration effect. The hydrodynamic retention has a small contribution to the polymer retention in the formation rock. In its bigger part it is a reversible process, due to decreasing the sizes of the polymer molecules and increasing the flow rate.

*Mechanical entrapment* occurs in pores which are surrounded by shrinkage smaller than the size of the macromolecules. Mechanical retention has a significant contributor to polymer loss in the porous media. It is partly irreversible but the amount of retained polymer is usually not high.

In most cases retention of the polymer used in EOR is considered instantaneous and mainly irreversible. However, due to prolonged continuous injection a few of the polymers can be released from the pore space.

Stability under the particular reservoir conditions (temperature, salinity, etc.) is an important characteristic of the polymer. Determination of the polymer type for EOR processes is based on the particular reservoir environment and the expected residence time of the polymer in the reservoir rock. Degradation of the polymers reflects in the loss of solution viscosity with the time. For example degradation of the polymer is directly proportional to the change in temperature – degradation rate increases with increasing the temperature. Also degradation can be caused by oxidative attack and bacterial attack. In order to decrease

the polymer degradation it is important to be selected a polymer that corresponds to the conditions in the reservoir.

Because of the size (bigger than water molecules), polymers cannot access some pores in the porous formation. The fraction of pore space in the porous rock, which cannot be contacted by the polymer solution, is called inaccessible pore volume (IPV). The magnitude of the IPV ranges from 1%-2% to 25%-30% for polymer flow injected in the porous media. This percent is based on both – type of the polymer and the type of the porous media. At every point in the porous formation, the accessible to polymers pore volume is  $(\phi_{sw}-\phi_{IPV})$ . For convenience it is defined as<sup>(13)</sup>:

$$\phi_e = \frac{\phi_{IPV}}{\phi} \quad (19)$$

Where:

$\phi_e$  – effective inaccessible pore volume;

$\phi_{IPV}$  – inaccessible pore volume;

$\phi$  - porosity.

Based on the poor water flood recovery, Nagani oil field is evaluated as a good candidate for polymer-augmented water flooding.

Polymer-augmented waterflooding is a process applied not only in cases of unfavorable mobility ratio but also in case when the reservoir heterogeneity primary in vertical direction is high. This can result in poor volumetric sweep efficiency. In polymer augmented waterflooding is used water solution of high-molecular-weight polymers in order to augment the waterflooding.

Selected polymer for the flooding process is partially hydrolyzed polyacrylamide (HPAM).

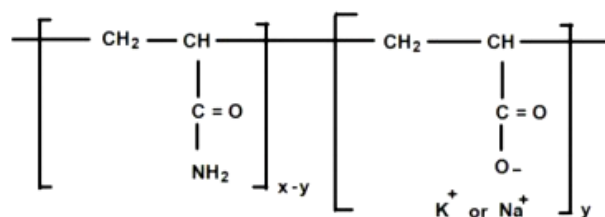


Fig. 15 Structure of HPAM (Aluhwal and Kalifa 2008)<sup>(14)</sup>

HPAM is a widely used synthetic polymer. It is created due to the process of polymerization of acrylic acid and acrylamide (nonionic) monomers, negatively charged in the carboxylate groups. Due to the strong interactions with the cations during the further hydrolysis process some amide groups (CONH<sub>2</sub>) are substituted by carboxyl groups (COO<sup>-</sup>). For decreasing the polymer adsorption on the solid surface is added a base (sodium hydroxide, potassium hydroxide, etc.). The degree of hydrolysis for HPAM varies between 15% and 35%. Retention for HPAM varies between 35 and 1000 lbm/acre-ft.

Polymer flooding is one of the chemical EOR methods which have major importance today. It involves an addition of polymers into the injected water.

## 2. Analytical method for EOR

Based on the available information from Nagani oil field interpolated to a linear analytical reservoir model, calculations for evaluating the profitability of the polymer-augmented waterflooding can be achieved. The main profit of the polymer injection is the improvement at the areal and volumetric sweep efficiency and accelerating the oil production. It is an ideal to apply for improving an unfavorable mobility ratio due to continuous polymer injection.

The efficiency of the polymer augmented flooding can be evaluated by comparing the oil production from it with oil production received from applying the ordinary waterflooding. Waterflooding consists of large amounts of water which are injected into the formation to sweep the remaining oil (oil left behind after the natural depletion of the reservoir) into the wellbore before being pumped into the surface. Calculations for both water flooding and polymer augmented flooding are based on the *frontal displacement theory* introduced by Buckley and Leverett (1942)<sup>(12)</sup>. This theory encompasses two equations: fractional flow equation and frontal advance equation.

Calculations are done by constructing a simple linear model of the reservoir with the implementation of both wells – one injector and one producer simultaneously. Characteristics of the reservoir like porosity, permeability, oil and water saturation and etc. are adopted from Nagani oil field. On the table below are introduced the reservoir characteristics.

Table 7 Parameters characterizing the theoretical reservoir model

<b>Reservoir parameters:</b>		
Wide (w)	500	ft
Cross sectional area (A)	15000	ft <sup>2</sup>
Length (L)	1000	ft
Depth (D)	6627.3	ft
Formation thickness (h)	30	ft
Temperature	140.9	<sup>o</sup> F
Porosity ( $\phi$ )	0.26	
Permeability (k)	495.9	mili darcy
Pore volume (PV)	694568.1211	bbl
Initial oil saturation ( $S_{oi}$ )	0.8	
Interstitial water saturation ( $S_{wi}$ )	0.2	
Connet water saturation ( $S_{wc}$ )	0.2	
Residual oil saturation ( $S_{or}$ )	0.6	
Residual water saturation ( $S_{wr}$ )	0.4	
Density of the oil ( $\rho_o$ )	875.3	kg/m3
Density of the water ( $\rho_w$ )	1020.3	kg/m3
Viscosity of the oil ( $\mu_o$ )	4	cp
Viscosity of the water ( $\mu_w$ )	0.4	cp
Volume formation factor of oil	1	
Vilume formation factor of water	1	
Injection rate ( $q_i$ )	1000	bbl/day
Apperent viscosity of the polymer solution ( $\mu_p$ )	4	cp

## 2.1 Calculations for waterflooding in a linear system

All of the calculations have been done in excel .The applied procedure for calculating the water flooding is summarized in this section.

Plotting the values of the relative permeability ratio over the water saturation in a semi-log scale and building an exponential tend-line gives the slope and the intercept values estimated by excel. Those values are used in the further calculations.

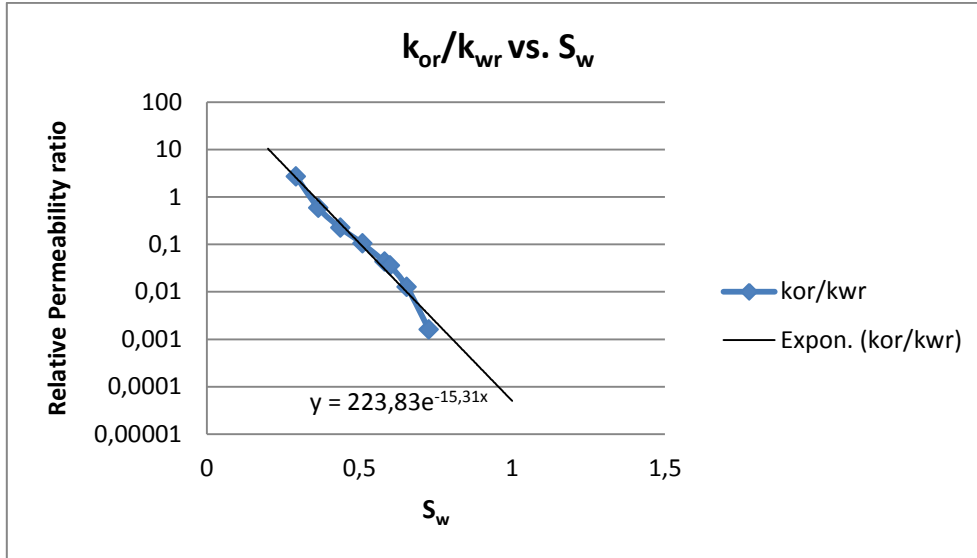


Fig. 16 Plot of the relative permeability ratio over the water saturation

$$\frac{k_{ro}}{k_{rw}} = a e^{bS_w}$$

From Fig.16 are received the values for the intercept  $a = 223.83$  and the slope  $b = -15.31$ .

For horizontal system due to which the gravity and capillary forces are negligible the fractional flow of water can be calculated as it follows<sup>(12)</sup>:

$$f_w = \frac{1}{1 + \left(\frac{\mu_w}{\mu_o}\right) a e^{bS_w}} \quad (20)$$

Where:

$f_w$  – fractional flow of water – dimensionless;

$e^{bS_w}$  – the exponential value of  $b$  multiplied with  $S_w$ .

Based on the results from this equation was built the fractional flow curve. The fractional flow curve is characteristically S-shaped and its limits (0 and 1) are assigned by the end points of the relative permeability curves. Important is the fact that any influence leading to upward shift into the curve will result in a less efficient displacement process. A tangent line was constrained to the fractional flow curve and from the point in which the tangent line touches the curve was obtained the value of frontal water saturation ( $S_{wf}$ ) and corresponding to leading edge of the water front ( $f_{wf}$ ) - Welge (1952)<sup>(12)</sup>.

There are two ways for estimation of the derivative values  $(df_w/dS_w)_{S_w}$  – graphically (from the tangent line) and numerically. The more accurate is the numerical method. It is the one used in the following calculations. Equation used for calculations is<sup>(12)</sup>:

$$\left(\frac{df_w}{dS_w}\right)_{S_w} = \frac{-\left(\frac{\mu_w}{\mu_o}\right) a b e^{bS_w}}{\left[1 + \left(\frac{\mu_w}{\mu_o}\right) a e^{bS_w}\right]^2} \quad (21)$$

The results received from equation (21) were plotted along with the fractional flow curve and introduced on the figure below. (Fig.17)

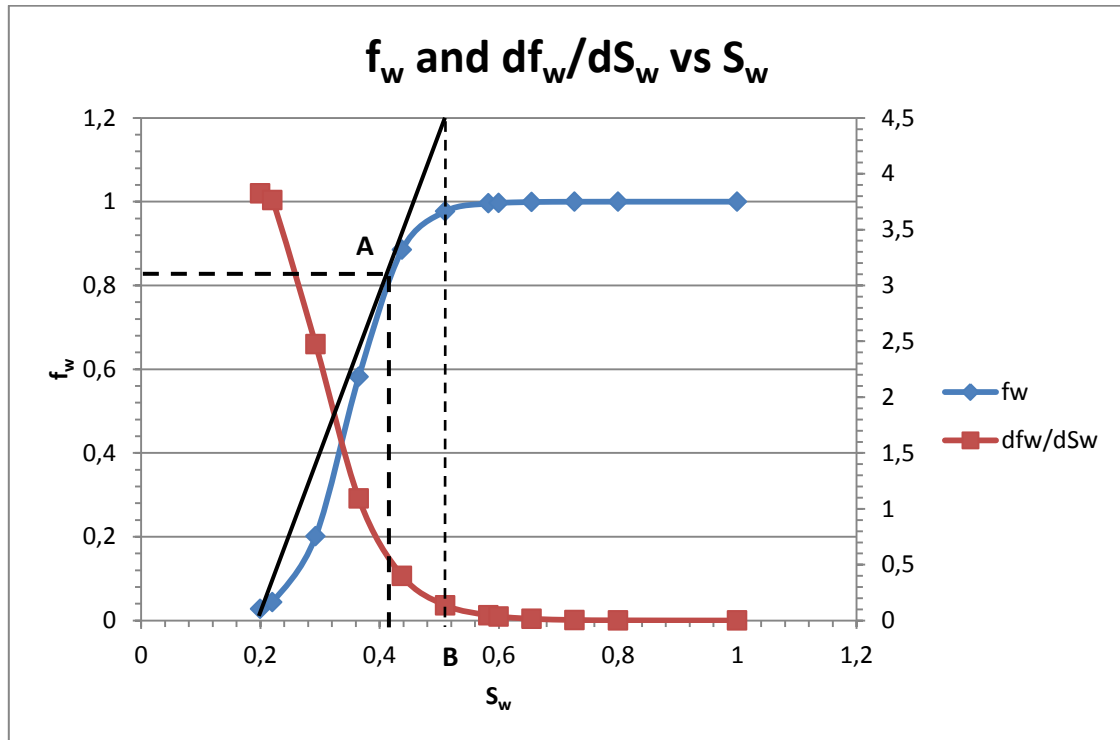


Fig. 17 Plot of the  $f_w$  and  $df_w/dS_w$  vs.  $S_w$  regarding the waterflooding

On Fig.17 are introduced graphically the results from equations (20) and (21). As it can be observed on the plot the start point of the tangent line is the interstitial water saturation ( $S_{wi}$ ). At point **A** on the plot is pointed out the location of the water breakthrough and respectively the values for  $S_{wf}$  and  $f_{wf}$ . At point **B** is pointed out the average water saturation behind the flood front after water breakthrough.

In order to estimate the water saturation behind the breakthrough point needs to be created a separate graph illustrating the fractional flow curve from the breakthrough point up to the  $f_w$  equal to 1. On that plot are drawn tangent lines to the fractional flow curve in order to be estimated the value of the water saturations and corresponding fractional flow behind the breakthrough point. Fractional flow value for the particular saturation is located at the point in which the tangent line crosses the y axes.

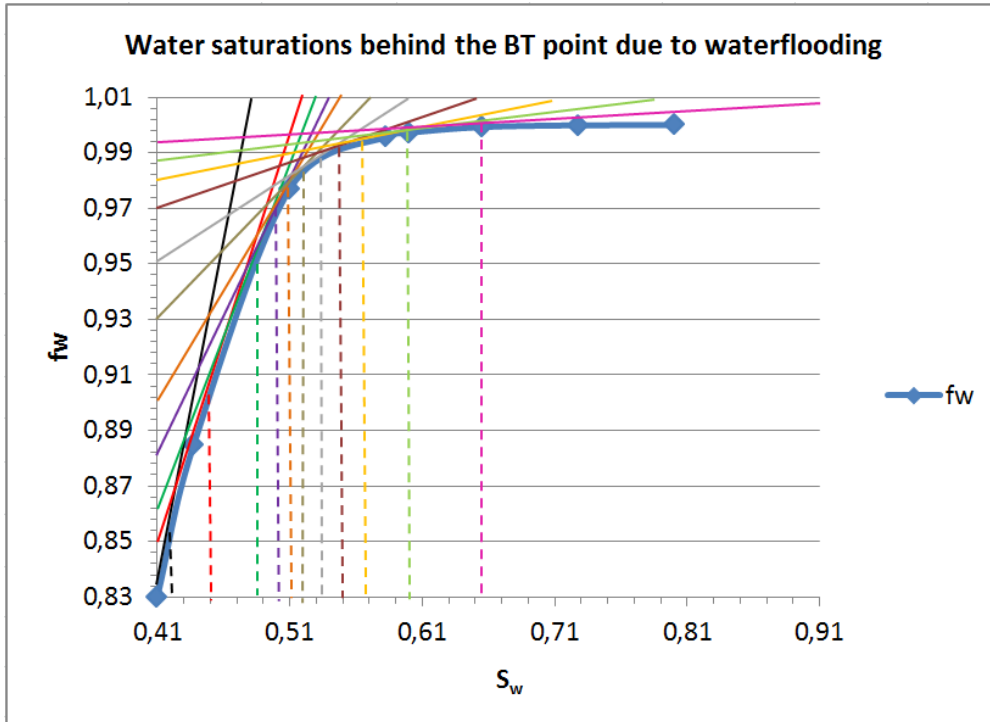


Fig. 18 Graphical evaluation of the water saturations located behind the breakthrough due to the waterflooding

From Fig. 18 were extracted eleven values, characterizing the water saturation and corresponding fractional flow behind the water breakthrough point. Those values are presented on the table below:

Table 8 Values received for the water  $S_w$  and  $f_w$  behind the behind the breakthrough point due to the waterflooding

$S_w$	$f_w$
0.42	0.834
0.45	0.85
0.48	0.862
0.49	0.882
0.51	0.9
0.52	0.93
0.535	0.95
0.55	0.97
0.57	0.98
0.6	0.986
0.655	0.994

The slope of the tangent line is calculated by the following equation (13):

$$f'_{wf} = \frac{(f_{wf} - f_{iw})}{(S_{wf} - S_{iw})} \quad (22)$$

Where:

$f'_{wf}$  – slope;

$f_{wf}$  – fractional flow of water at the flood-front saturation;

$f_{iw}$  – fractional flow of water at interstitial water saturation;

$S_{wf}$  – flood-front saturation;

$S_{iw}$  – interstitial water saturation.

On Table 9 (below) are summarized the main values characterizing the flood front at the water breakthrough point estimated from equations (20), (21) and (22). The values for fractional flow and estimated derivatives were calculated in excel file.

Table 9 Values of the parameters at the breakthrough point

Parameters	Received values
$f'_{wf}$	3.95
$S_{wf}$	0.41
$f_{wf}$	0.83
$df_w/dS_w$	0.59

Due to the waterflooding process in the reservoir are formed saturation zones. All saturations encompassed in the region – between connet water saturation ( $S_{wc}$ ) and  $S_{wf}$  are moving with the same velocity as a function of time and distance. That was found by Terwilliger et al. (1951) (12), regarding the lower range of water saturation. As a result of that the shape of the water saturation profile will remain the same with time. The reservoir flooded zone with low range of water saturations ( $S_{wc}$  to  $S_{wf}$ ) is termed as **stabilized zone**. Other indentified saturation zone corresponds to the saturations in the range from  $S_{wf}$  to  $(1-S_{or})$  and it is termed as **nonstabilized zone**. Based on core flood data was determined that there is a **shock front**. In the shock front the water saturation abruptly increases from  $S_{wc}$  to  $S_{wf}$ . Behind the flood front the saturation starts to increase until it reaches the maximum of  $(1-S_{or})$ . Based on that,  $S_{wf}$  is said to be the water saturation of the front.

For estimation of the water saturation profile regarding the distance and time is used the *frontal advanced equation equations* (12):

$$(x)_{sw} = \left( \frac{5.615 i_w t}{\phi A} \right) \left( \frac{df_w}{dS_w} \right)_{S_{wf}} \quad (23)$$

The frontal advanced equation allows to be calculated the location of each saturation regarding the time (t). Before applying equation (23), first have to be estimated the time – distance relation. This relation is illustrated with the following equations<sup>(12)</sup>:

$$t_D = \frac{x_D}{f'_w} \quad (24)$$

For

$$x_D = 1$$

$$t_D = \frac{1}{f_w}$$

Where:

$t_D$  – dimensionless time;

$x_D$  – dimensionless distance from origin.

The dimensionless distance can vary in the ratio between 0 and 1.  $x_D=1$  corresponds to the end of the linear system. The dimensionless distance is calculated by the following equation <sup>(13)</sup>:

$$x_D = f_w t_D \quad (25)$$

Time in days instead of dimensionless time is evaluated by:

$$t = \left( \frac{V_p}{q_i} \right) * t_D \quad (26)$$

Where:

$V_p$  – pore volume;

$q_i$  – injection rate.

Due to the application of the frontal advanced equation have been calculated the water saturation profile regarding the time for a particular location. The first series of calculations are based on  $x_D=1$ . From there it is calculated the corresponding time and location. Results are introduced summarized below.

**Table 10 Calculation of the water saturation profile**

$S_w$	$df_w/dS_w$	$(x)_{BT}S_w$	$(x)_1S_w$	$(x)_2S_w$	$(x)_3S_w$
0,41	0,592929	150,0183	112,5137	75,00915	37,50458
0,42	0,514639	130,2099	97,65746	65,10497	32,55249
0,45	0,333614	84,40834	63,30625	42,20417	21,10208
0,48	0,214255	54,20915	40,65686	27,10457	13,55229
0,49	0,184584	46,70187	35,0264	23,35093	11,67547
0,51	0,136777	34,60621	25,95466	17,3031	8,651552
0,52	0,117662	29,76979	22,32734	14,8849	7,442448
0,535	0,093817	23,73677	17,80258	11,86838	5,934192
0,55	0,074756	18,91409	14,18557	9,457045	4,728522
0,57	0,055181	13,96141	10,47106	6,980706	3,490353
0,6	0,034952	8,843329	6,632497	4,421665	2,210832
0,655	0,015098	3,819883	2,864912	1,909942	0,954971
<b>Time (days)</b>		<b>175,7</b>	<b>131,8</b>	<b>87,8</b>	<b>43,9</b>

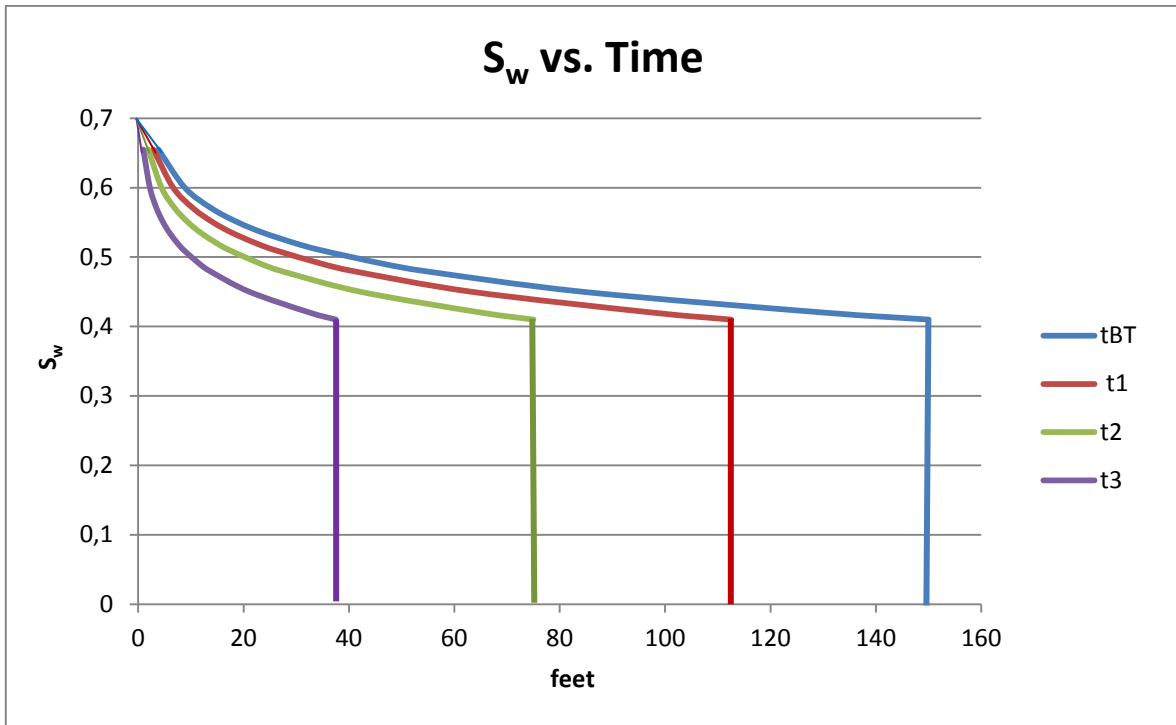


Fig. 19 Water saturation profile as a function of distance (feet) and time (days)

As it can be observed from Fig. 19 and Table 10 the time estimated for the breakthrough point of the water flood front is 175,7 day. The corresponding location is calculated to be equal to 150 feet from the water injection well, which corresponds to less than half of the distance between the injection and production well.

Regarding the results received so far have been derived oil recovery calculations for estimating the waterflood performance. For evaluating the waterflood performance, first of all was calculated the average water saturation. It is necessary for calculating some of the parameters. The equation applied for estimating the average water saturation at any time after the breakthrough is calculated from the Welge equation (13).

$$\bar{S}_w = S_w + t_D(1 - f_w) \quad (27)$$

Where

$\bar{S}_w$  - average water saturation in the swept area.

Afterwards have been calculated the following parameters characterizing the waterflood performance. Those calculations include:

- Cumulative pore volume of the injected water ( $Q_i$ );
- Original oil in-place (OOIP);
- Cumulative oil production ( $N_p$ );
- Oil rate at reservoir conditions ( $Q_o$ );
- Water rate at reservoir conditions ( $Q_w$ );
- Water- Oil ratio (WOR);
- Displacement efficiency ( $E_d$ );
- Cumulative water injected ( $W_{inj}$ );

Cumulative pore volume of the injected water ( $Q_i$ ) is defined at the time when the water saturation reaches the water saturation on the producing well. It is the reciprocal of the slope of the tangent line and is calculated by the following equation<sup>(12)</sup>:

$$Q_i = \frac{1}{\left(\frac{df_w}{dS_w}\right)_{S_{w2}}} \quad (28)$$

Original oil in-place (OOIP) is calculated by<sup>(13)</sup>:

$$OOIP = N_s = \frac{V_p(1 - S_{wi})}{B_o} \quad (29)$$

Cumulative oil production ( $N_p$ ) is calculated due to the lack of gas by the following equation<sup>(13)</sup>:

$$N_p = \frac{t_{Df}V_p}{B_o} \quad (30)$$

Oil rate at reservoir conditions ( $Q_o$ ) is calculated before (30) and after (31) the water breakthrough<sup>(12)</sup>:

$$Q_o = \frac{q_i}{B_o} \quad (31)$$

And

$$Q_o = \frac{q_i(1 - f_w)}{B_o} \quad (32)$$

Water rate at reservoir conditions ( $Q_w$ ) corresponds to the surface water rate because of the lack of gas in the reservoir<sup>(12)</sup>:

$$Q_w = \frac{q_i f_w}{B_w} \quad (33)$$

Water- Oil ratio (WAR) is calculated by<sup>(12)</sup>:

$$WOR = \frac{B_o}{B_w \left( \frac{1}{f_{w2}} - 1 \right)} \quad (34)$$

Displacement efficiency ( $E_d$ ) is calculated for each selected value of the water saturation at the production well ( $S_{w2}$ ) by the following equation<sup>(12)</sup>:

$$E_d = \frac{\overline{S_{w2}} - S_{wi}}{1 - S_{wi}} \quad (35)$$

Cumulative water injected ( $W_{inj}$ ) is calculated by<sup>(12)</sup>:

$$W_{inj} = q_i t_{BT} \quad (36)$$

## 2.1.2 Results

Results from the already mentioned equations are introduced in the table below.

Table 11 Results for reservoir performance until the point of water breakthrough

<b>Reservoir performance up to the point of water breakthrough</b>					
<b>t (days)</b>	<b><math>W_{inj}=q_i t</math></b>	<b><math>N_p=W_{inj}/B_o</math></b>	<b><math>Q_o=i_w/B_o</math></b>	<b><math>Q_w</math></b>	<b>WOR</b>
175	175000	175000	1000	0	0
175,7**	836200	836200	170	830	4,88

\*\* water breakthrough

Table 12 Reservoir performance after the water breakthrough

<b>Reservoir performance after the water breakthrough</b>						
<b>t (days)</b>	<b>W<sub>inj</sub> (bbl)</b>	<b>N<sub>p</sub> (STB)</b>	<b>Q<sub>o</sub> (STB/day)</b>	<b>Q<sub>w</sub> (STB/day)</b>	<b>WOR (STB/STB)</b>	<b>E<sub>D</sub></b>
175,7341	175734,1029	175734,1	170	830	4,882352941	0,315625
183,2194	183219,4084	183219,4	166	834	5,024096386	0,326875
204,2847	204284,7415	204284,7	150	850	5,666666667	0,359375
225,6138	225613,7748	225613,8	138	862	6,246376812	0,393125
228,3727	228372,7382	228372,7	118	882	7,474576271	0,399375
239,2401	239240,1306	239240,1	100	900	9	0,41875
238,9912	238991,1815	238991,2	70	930	13,28571429	0,421875
244,9267	244926,6532	244926,7	50	950	19	0,434375
250,6174	250617,3633	250617,4	30	970	32,33333333	0,446875
262,2349	262234,9029	262234,9	20	980	49	0,46875
281,7721	281772,0572	281772,1	14	986	70,42857143	0,504375
317,9361	317936,1118	317936,1	6	994	165,6666667	0,570625

From the tables above is observed the change in the production regarding the time. On table 11 depicted that the volume of oil displaced at the water breakthrough is sized up to the volume of injected water. That is explained by Buckley-Leveret theory which implies that mass is conserved<sup>(12)</sup>.

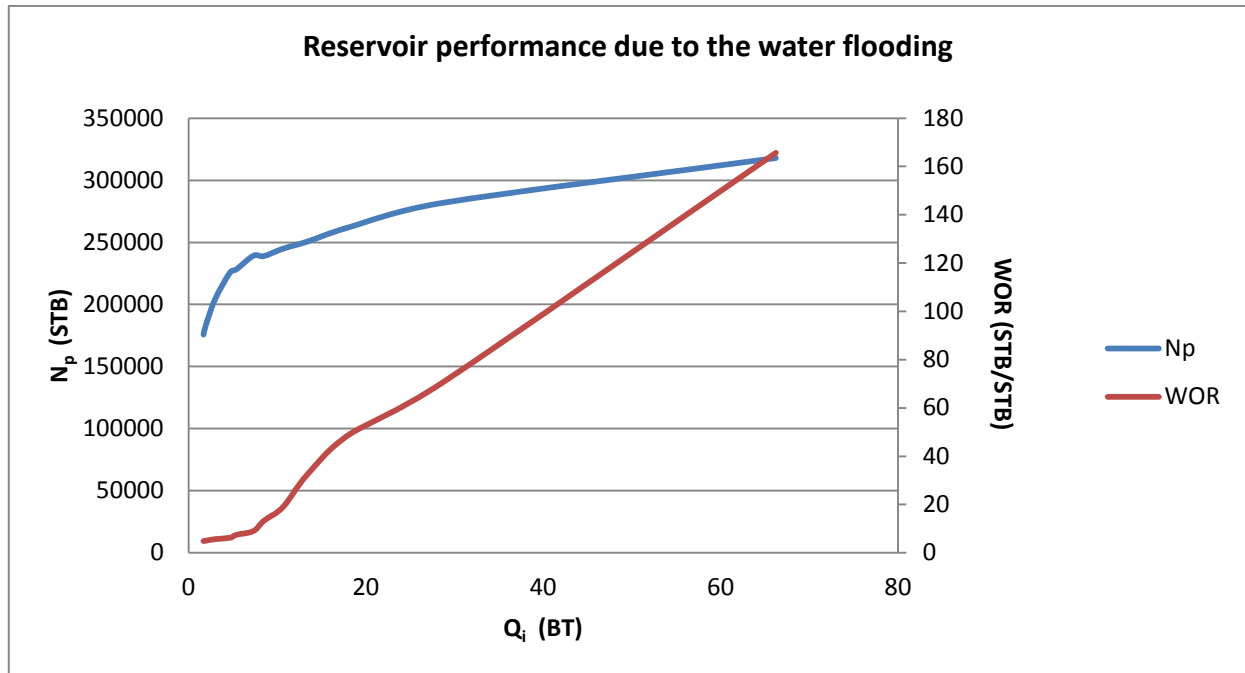


Fig. 20 Reservoir performance due to the waterflooding

Results received for cumulative oil production and water-oil ratio (WOR) are presented graphically on Fig.20. According to the graph after the breakthrough point WOR increases fast until it crosses the cumulative oil production curve. At that point main production is consisted mainly of water. The high rate with which the WOR increases can be referred to the unfavorable mobility ratio. It is also the reason for the early breakthrough. The improvement in the mobility ratio will lead to a delay in the water breakthrough which will improve the displacement efficiency.

## 2.2 Calculations for Polymer-Augmented Waterflooding in linear system

All of the calculations have been done in excel. The applied procedure for calculating the polymer-augmented waterflooding is introduced in this section. For the calculations was used the principle for continuous polymer injection. Calculating pattern is similar to the one, applied for waterflooding.

End points relative permeability data is used for calculating the mobility ratio. Based on the size of the mobility ratio is estimated the needed apparent viscosity of the polymer. End point mobility ratio is estimated by equation (10).

$$M = \frac{1 * 4}{0.4 * 0.9} = 11$$

It is clearly seen that the mobility ratio is unfavorable.

$$\lambda = \frac{4}{0.4} = 10$$

Therefore

$$\mu_o = 10 (\mu_w)$$

Due to improve the mobility ratio is assumed 300ppm polymer with apparent viscosity of 4 cp in order to adjust the mobility ratio to be lower or equal to 1. The retention of the selected amount of polymer is 17.5mg/g at 300ppm so the polymer retention ( $D_p$ ) is equal to 0.424<sup>(13)</sup>. Also assumed is the value of inaccessible pore volume (IPV) of the system to be 0.25 (13). Thus

$$-\phi_e + D_p = 0.174$$

Values fractional flow curve are derived using the approach explained in the previous section by applying equation (20). For estimating the properties of the polymer flood front  $-S_w^*$  and  $f_w^*$  has been built a tangent line which intersects the waterflooding fractional flow curve in point which reflects location of the oil bank front. From that point are obtained the values for water saturation ( $S_{w1}$ ) and fractional water flow ( $f_{w1}$ ).

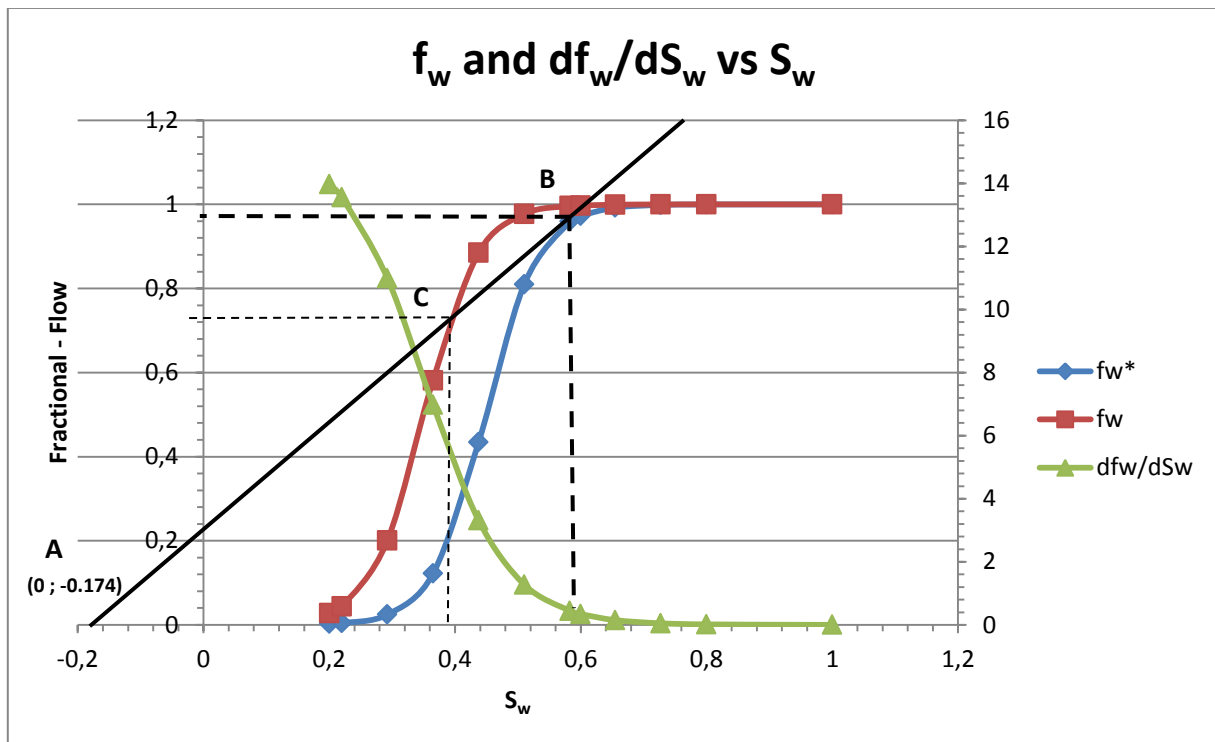


Fig. 21 Plot of the  $f_w$  and  $df_w/dS_w$  vs.  $S_w$  for polymer-augmented waterflooding

Fig. 21 illustrates the results from equations (20) and (21) regarding the polymer-augmented flooding along with the fractional flow curve computed for waterflooding. Values estimated for  $S_{wf}$ ,  $f_{wf}$  and  $f_w$  correspond to the values of water front for the polymer-augmented waterflooding. At point **A** on the plot is depicted the start point of the tangent line. As opposed to the tangent line built for the water flooding it does not start from  $S_{wi}$ . The start point coordinates (0 ; -0,174) were estimated based on  $-\phi_e + D_p$ . This is because for the polymer flood in the beginning of injections, the polymer condition is not certain. At point **B** is pointed out the location of the polymer flood front. It is characterized with water saturation and fractional

flow of the polymer front –  $S_w^*$  and  $f_w^*$ . At point **C** are located the oil bank water saturation ( $S_{w1}$ ) and corresponding to it oil bank fractional flow ( $f_{w1}$ ).

In order to estimate the water saturation behind the polymer front breakthrough point needs to be created separate graph illustrating the fractional flow curve from the breakthrough point up to the  $f_w$  equal to 1. On that plot are drawn tangent lines to the fractional flow curve in order to be estimated the value of the water saturations and corresponding fraction flow behind the polymer breakthrough point. Fractional flow for the particular saturation is located at the point in which the tangent line crosses the y axes.

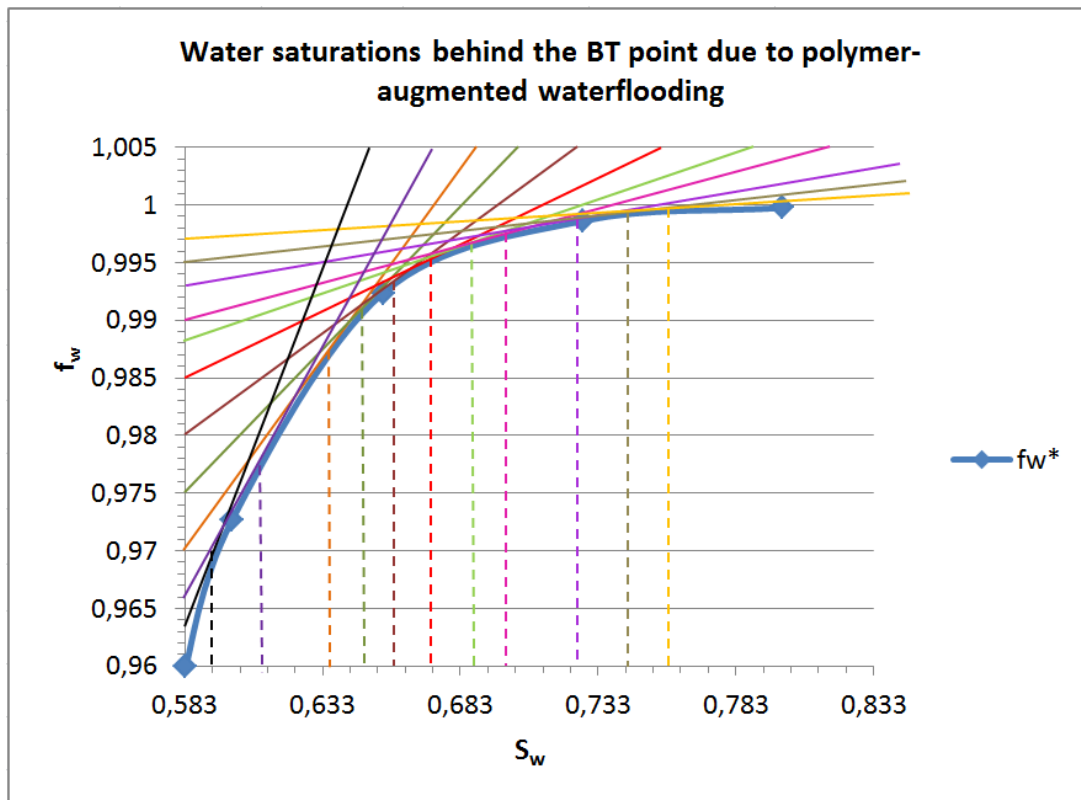


Fig. 22 Graphical evaluation of the water saturations located behind the breakthrough due to the polymer-augmented waterflooding

From Fig. 22 were extracted eleven values, characterizing the water saturation and corresponding fractional flow behind the polymer breakthrough point. Those values are presented on the table below:

Table 13 Values received for the water  $S_w^*$  and  $f_w^*$  behind the breakthrough point due to the polymer-augmented waterflooding

$S_w^*$	$f_w^*$
0,586	0,963
0,595	0,966
0,634	0,967
0,648	0,975
0,658	0,98
0,673	0,985
0,686	0,987
0,688	0,99
0,697	0,993
0,743	0,995
0,758	0,996

The observed location of the oil bank indicates for low-tensional flood. Regarding the established consistency of the saturations-  $S_{wf} < S_{w1} < S_w^*$  improvement in the oil bank front is needed to be made. The difference between  $S_{wf}$  and  $S_{w1}$  is said to be quite small. Regarding the value of  $S_{w1}$  used in this project is assumed to be bigger than  $S_{wf}$  with 0.008 (13). Based on that was estimated graphically  $f_{w1}$ . On the table below are introduced the values estimated from Fig. 21 with the corrections regarding oil bank front.

Table 14 Graphically estimated values characterizing the polymer, oil and water bank fronts

Polymer bank		Oil bank		Water bank	
$f_{wf}^*$	2.5	$f_{w1}$	3.85	$f_{wf}$	3.95
$f_w^*$	0.96	$f_{w1}$	0.84	$f_{wf}$	0.83
$S_w^*$	0.583	$S_{w1}$	0.418	$S_{wf}$	0.41
$(df_w/dS_w)_{S_w^*}$	0.442	$(df_{w1}/dS_{w1})_{S_{w1}}$	4.15	$(df_{wf}/dS_{wf})$	0.59

For estimating the location of the polymer front regarding the distance and time is used the *frontal advanced equation equations* <sup>(12)</sup>. The method of calculations is the same as the one used in the waterflooding calculations. Received results due to the application of equations (23), (24), (25) and (26) are introduced below.

Table 15 Calculations of polymer saturated profile

$S_w^*$	$(df_w/dS_w)^*$	$(x)_{BT}S_w^*$	$(x)_1S_w^*$	$(x)_2S_w^*$	$(x)_3S_w^*$
0,583	0,44234931	176,4789	132,3592	88,23947	44,11974
0,586	0,42304043	168,7755	126,5816	84,38775	42,19388
0,595	0,36990299	147,5759	110,6819	73,78794	36,89397
0,634	0,20583455	82,11941	61,58956	41,0597	20,52985
0,648	0,16655571	66,44879	49,83659	33,22439	16,6122
0,658	0,14313315	57,10416	42,82812	28,55208	14,27604
0,673	0,11398256	45,47429	34,10572	22,73715	11,36857
0,686	0,09353728	37,31748	27,98811	18,65874	9,329369
0,688	0,09073329	36,1988	27,1491	18,0994	9,0497
0,697	0,0791146	31,56343	23,67257	15,78171	7,890857
0,743	0,0392226	15,64818	11,73614	7,824092	3,912046
0,758	0,03119098	12,4439	9,332926	6,221951	3,110975
time (days)		277.1	207.8	138.5	69.2

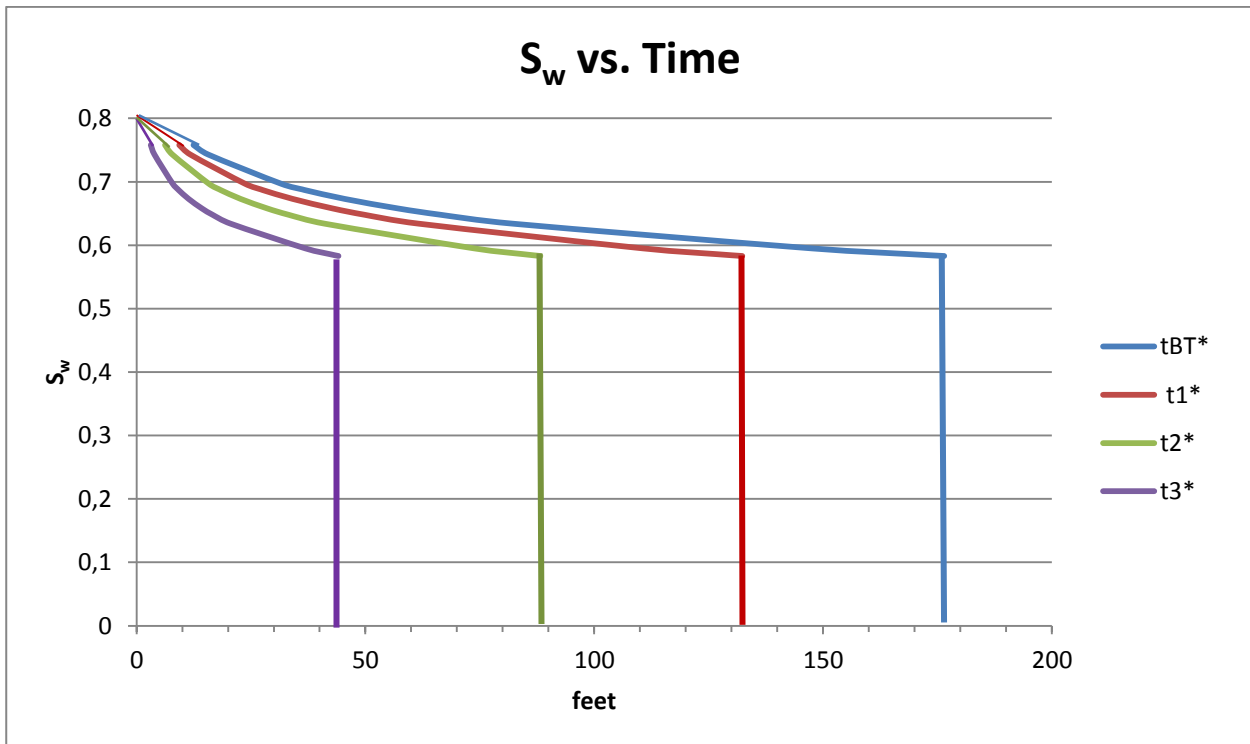


Fig. 23 Polymers front profile as a function of distance (feet) and time (days)

As it can be observed from Fig. 23 and Table 15 the time needed for the polymer front to get to the breakthrough point is 277.1 day. Location of the breakthrough is estimated to be equal to 176.4 feet from the water injection well.

Regarding the results received so far have been derived oil recovery calculations for estimating the polymer-augmented waterflooding performance. For evaluating the waterflood performance, first of all were calculated the average water saturation. Calculating the average saturation is necessary in order to locate the saturation of the three fronts - water front, oil front and polymer front. Also it is used for calculating some of the parameters. The equation applied for estimating the average water saturation at any time after the breakthrough is calculated from the Welge equation<sup>(13)</sup>- equation (27).

Saturation from  $S_{wf}$  to  $S_{w1}$  is uniform based on the difference in the velocities between the zones.

Afterwards have been calculated the following parameters characterizing the polymer-augmented waterflood performance. Those calculations include:

- Cumulative pore volume of the injected water ( $Q_i$ ) – equation (28)
- Cumulative oil production ( $N_p$ )- equation (30);
- Oil rate at reservoir conditions ( $Q_o$ )- equations (31)and (32);
- Water rate at reservoir conditions ( $Q_w$ )- equation (33);
- Water- Oil ratio ( $F_{wo}$ ) (13);
- Displacement efficiency ( $E_d$ )- equation (35)

For calculating the cumulative oil production for water, oil and polymer front is used again equation (30) regarding the fact that there is no gas in the system.

For estimation of the water –oil ratio has been used the following equation<sup>(13)</sup>:

$$F_{wo} = \frac{f_w}{1 - f_w} \quad (37)$$

This equation – (37) gives the same results as equation (34).

## 2.2.2 Results

On the table below are introduced the events at the end of the system. Those results depict the oil recovery due to the polymer-augmented waterflooding.

Table 16 Oil recovery calculations due to the polymer-augmented waterflooding

<b>Arrival of the water bank</b>	<b>S<sub>w</sub> (av.)</b>	<b>Ed</b>	<b>Q<sub>i</sub> (BT)</b>	<b>N<sub>p</sub> (STB)</b>	<b>q<sub>o</sub> (STB/day)</b>	<b>q<sub>w</sub> (STB/day)</b>	<b>t (days)</b>	<b>F<sub>wo</sub></b>
	0,4525	0,315625	1,686541	175734,1	170	830	175,7341	4,882353
<b>Arrival of the oil bank</b>	<b>S<sub>wi</sub> (av.)</b>	<b>Ed</b>	<b>Q<sub>i</sub> (BT)</b>	<b>N<sub>p</sub></b>	<b>q<sub>o</sub></b>	<b>q<sub>w</sub></b>	<b>t (days)</b>	<b>F<sub>wo</sub></b>
	0,459524	0,32440476	0,24087	180257	160	840	180,257	5,25
<b>Arrival of polymer front</b>	<b>S<sub>w</sub>* (av.)</b>	<b>Ed</b>	<b>Q<sub>i</sub> (BT)</b>	<b>N<sub>p</sub></b>	<b>q<sub>o</sub></b>	<b>q<sub>w</sub></b>	<b>t (days)</b>	<b>F<sub>wo</sub></b>
	0,598958	0,49869792	2,260657	277103,7	40	960	277,1037	24
<b>Polymer injection</b>	0,608515	0,51064382	2,36384	422655,2	37	963	422,6552	26,02703
	0,615942	0,51992754	2,703411	427813,7	34	966	427,8137	28,41176
	0,655636	0,56954498	4,858271	455383,9	33	967	455,3839	29,30303
	0,664615	0,58076923	6,003997	461620,7	25	975	461,6207	39
	0,671429	0,58928571	6,986501	466352,9	20	980	466,3529	49
	0,683249	0,60406091	8,773272	474562,8	15	985	474,5628	65,66667
	0,695035	0,61879433	10,69092	482749,5	13	987	482,7495	75,92308
	0,694949	0,61868687	11,02131	482689,8	10	990	482,6898	99
	0,701913	0,62739174	12,63989	487526,7	7	993	487,5267	141,8571
	0,746734	0,68341709	25,4955	518657,4	5	995	518,6574	199
0,761044	0,70130522	32,06055	528597	4	996	528,597	249	

The results regarding the reservoir performance due to the polymer augmented waterflooding are introduced graphically on the figure below:

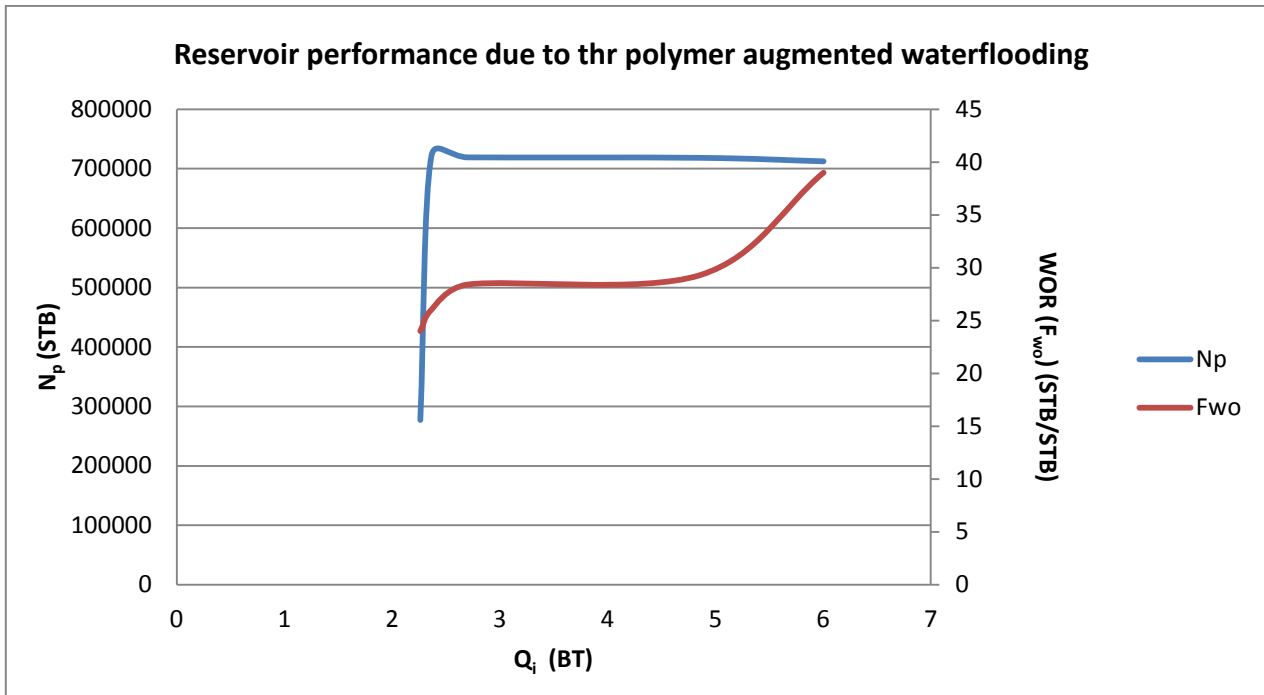


Fig. 24 Reservoir performance due to the polymer augmented waterflooding

On Fig.24 is depicted in logarithmic scale the reservoir performance due to the polymer –augmented waterflooding.

The results received assessed from Table 16 and Fig. 24 illustrating that the increase in the WOR has a relative low rate which contributes to more stable displacement process. On Fig. 24 is depicted the rapid increase in the WOR after the breakthrough point and following plateau region subsequent by gradual increase in WOR. This increase in the WOR can be related with decreased viscosity of the polymer which leads to increase in the mobility of the water.

### 2.3 Evaluation of the additional oil recovery

For each of the both flooding mechanisms was evaluated and introduced by tables the cumulative oil regarding the time. In order to estimate the additional oil recovery it is needed some recalculations to be done.

Due to the waterflooding and polymer augmented flooding were calculated and introduced the results regarding the oil production for particular time and corresponding location. As it was already established according to the received results in table 12 (reservoir performance due to waterflooding) and table 16 (reservoir performance due to polymer augmented waterflooding) the days corresponding to the cumulative oil production are different for both cases. The additional oil recovery can be calculated only if there is information for the oil production in common days. In order to be observed the additional oil recovery there are needed to be done recalculations regarding water saturation. For estimating the additional oil recovery has to be calculations have to be done in two steps. First step is to be determined the production by polymer-augmented waterflooding at the water flood breakthrough time. This is done by

calculating the average water saturation after the water-flood front and before the oil bank, by the following equation (13):

$$\bar{S}_{w2} = \frac{(S_{wf} - x_{D1})S_{w1}}{1 - x_{D1}} - \frac{t_{D2}(f_{wf} - f_{w1})}{1 - x_{D1}} \quad (38)$$

Received value from equation (38) is implemented in the equation for calculating the water saturation for the polymer flood at water breakthrough time (13).

$$\bar{S}_{w3} = S_{w3}x_{D3} + S_{w1}(x_{D1} - x_{D3}) + (1 - x_{D1})\bar{S}_{w2} \quad (39)$$

Where for the both (38) and (39):

$\bar{S}_{w3}$  – average water saturation for the polymer flood;

$S_{w1}$  – water saturation at the oil bank;

$x_{D1}$  – the location of the oil bank at the breakthrough time;

$S_{w3}$  – water saturation of the polymer bank;

$x_{D3}$  – location of the polymer bank at breakthrough time.

The received result from equation (39) is used for calculating the oil production by<sup>(13)</sup>:

$$OOIP = N_p = \frac{V_p(\bar{S}_{w2} - S_{iw})}{B_o} \quad (40)$$

The second step is to calculate the waterflooding production at the polymer-augmented waterflooding breakthrough time. This is done by the following two equations<sup>(13)</sup>:

$$S_{w3} = \frac{S_{w1} + (t_{D3} - t_{D1})(S_{w2} - S_{w1})}{(t_{D2} - t_{D1})} \quad (41)$$

And

$$\bar{S}_{w3} = \frac{\bar{S}_{w1} + (t_{D3} + t_{D1})(\bar{S}_{w2} - \bar{S}_{w1})}{(t_{D2} - t_{D1})} \quad (42)$$

Where:

$t_{D1}$  – dimensionless time regarding oil bank;

$t_{D2}$  – dimensionless time regarding water bank.

The received value from equation (42) implemented in equation (40) for calculating the production. The values for the additional oil recovery are reflecting the difference in production between the waterflooding and polymer-augmented waterflooding. Results, obtained for the additional oil recovery are introduced on the table below:

Table 17 Results for additional oil recovery

t (days)	Waterflooding (STB)	Polymer augmented waterflooding (STB)	Additional recovery
175,73*	175734,10	0,00	-175734,10
183,22	183219,41	378032,88	194813,47
204,28	204284,74	177775,69	-26509,05
225,61	225613,77	164532,32	-61081,45
228,37	228372,74	163676,86	-64695,87
239,24	239240,13	161085,71	-78154,42
238,99	238991,18	161134,34	-77856,84
244,93	244926,65	160076,92	-84849,73
250,62	250617,36	159230,63	-91386,74
262,23	262234,90	157867,70	-104367,20
277,10**	271859,04	277103,74	5244,70

\*Water front breakthrough

\*\*Polymer front breakthrough

Due to the assessed values from Table 17 can be concluded that due to the time of polymer breakthrough there is neglected additional recovery. This result reflects the fact that due to the short period of time for water production after the polymer breakthrough the values for water flooding at polymer-augmented flooding breakthrough cannot be assessed. As a result the received values for additional oil recovery are inconclusive.

The results received due to the analytical calculations are based on a lot of assumptions. In order to be checked their accuracy they need to be implemented into the simulation model.

### 3. Implementation of Polymer-Augmented waterflooding in Nagani oil field

Implementation of the selected enhanced oil recovery method in Nagani oil field where the objective was to observe the improvements in the oil recovery based on received additional oil production and the level at which those results correspond to the one, calculated based on the analytical approach.

Applying the polymer-augmented waterflooding in Nagani oil field needed the derived values, in order for the analytical calculations to be integrated in Eclipse data file of the reservoir model.

Inferring that Nagani oil field was in production for six years and with the consequent validation of the reservoir model by the process of history matching, all led to the creation of a restart file, which served the purpose of introducing the forecast for the field behavior in the next 10 years to come. In the latter (restart file) production and injection wells were additionally inputted, whose location was selected based on the direction of the water flux.

Due to that two simulation cases where the numerical outcomes were compared in order to assess and situate the improvement in the oil production from the field.

On the table below are compared the results from both cases of numerical simulation.

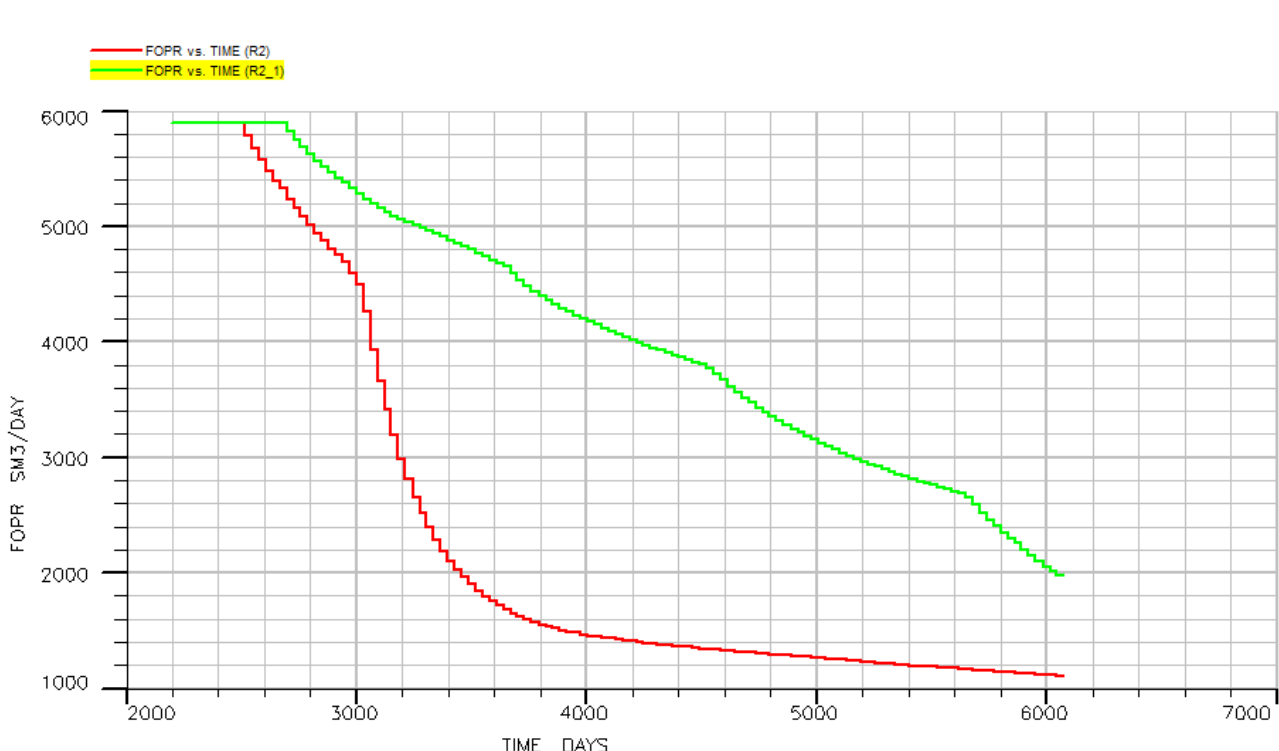


Fig. 25 Comparison of the results received from waterflooding and vicious flooding: with the green line is depicted the improved field oil production rate (FOPR) due to the increased viscosity and with red line is depicted FOPR due to water flooding.

On Fig. 25 is illustrated the improvement in the field oil production due to the increased viscosity of the brine. Due to the laboratory experiments with the polymer solutions as it was mentioned earlier in this report was created a polymer solution which exceeds the viscosity of the oil in the reservoir regarding the temperature (Appendix A). Based on that, the value of the polymer solution viscosity was implemented into the simulator in order to be observed the changes in the field behavior. Due to the injection of high viscous brine was observed also an increase in the reservoir pressure.

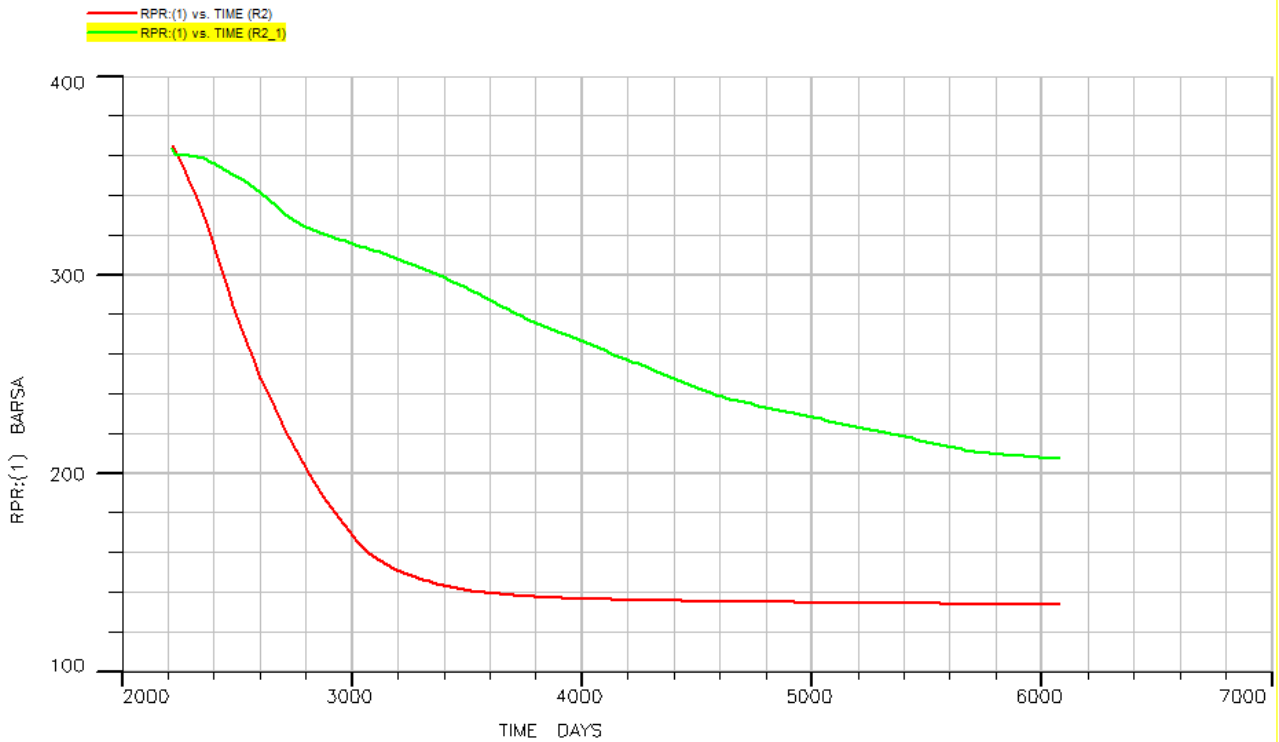


Fig. 26 Change into reservoir pressure due to the injection of high viscous brine compared with the water injections: with the green line is depicted improved reservoir pressure (RPR) due to the increased viscosity and with the red line is depicted RPR due to water flooding.

## Conclusion

During the project execution of several force ranking reservoir attributes and characteristics were computed. The main purpose of such was to adequately estimate the best-case scenario for applying an enhanced oil recovery (EOR) method in the particular reservoir succession. By engineering calculations and screening criteria investigation was concluded that the most suitable of all EOR methods for the specific case was the polymer flooding one. The latter is applied usually for oil viscosities larger than 10 cP and precise control of the mobility ratio, as this reservoir includes for its successful methods (Table 2). This report proves equally by striving towards emphasizing on to what extent the EOR procedure may be applicable and efficient for this reservoir and summarizing the overlapping of its parameters. For doing so, and embedding the polymer method to the specific reservoir, an analytical method was created with several assumption mechanisms used in prior of the calculations of the additional oil recovery. Its outcomes are skillful but cannot be approved until any further simulation is executed. However, it provides a critical overview and theoretical notion/idea for expected future results. This method is based on a simple linear reservoir, which serves as a comparison case, where the real data can be applied. Moreover, the reservoir parameters from the Nagani oil field which were proved as consistent were mimicked in the executed simple model, along with some assumptions. The derived values for the polymer concentration of 300 ppm and the retention time (13) were used due to insufficient laboratory experiments for the reservoir rock. In depth interpretation of the results led to the conclusion that the additional oil recovery calculated does not corroborate to the expected outcomes, and is not in full agreement with the values for the model.

As the model finds itself pendent and incomplete, the interpretation is mainly based upon Nagani Oil Field, in order to estimate to what extent the recovery is enhanced with the polymer injection. Furthermore the two empirical laboratory experiments conducted - the first of which includes the realistic justifications of the viscosity calculation of the dead oil by the mathematical approach previously done, and second build upon the gradual increasing concentration of the polymer and the relation to it with the thickening (viscosity increasing) of the medium, showed consistency in the polymer viscosity. The solution received was with viscosity close to the oil (4.00) one, as the temperature was increased to 60.5°C, where an obvious shear thickening was expressed from 4.14 cP (Appendix A). This infers for the possibility of achieving favorable mobility ration value of less than 1.

For the arising of technical incapability a decision was made to check at what extent a viscosity of 4.14 cp would supplementary improve the actual flow rate production of the reservoir. This was achieved by increasing the brine viscosity to the equal value of the polymer one (Figure 1 and 2), where a clear trend of increasing production and pressure in the reservoir was viewed with the injection of more viscous solution.

All the achieved calculations and models can be further optimized in future with the capability of developing a simulation model, which was constrained in participating in this thesis due to the difficulties experienced with acquiring the license for the Eclipse simulator. Moreover, amid the calculations some uncertainties exist, which the author is aware of, and will try to transpose or remove further on.

**Appendix A - Laboratory measurements**

## Table of Figures

Fig. 1 Hubbert curve <sup>(1)</sup> .....	5
Fig. 2 Realistic model of oil and gas production <sup>(1)</sup> .....	6
Fig. 3 Hierarchy of oil production <sup>(2)</sup> .....	7
Fig. 4 Percentage of OOIP extracted through primary and secondary recovery .....	8
Fig. 5 Distribution of two immiscible fluids at pore scale (6) .....	11
Fig. 6 Relative Permeability as a function of wetting fluid saturation for Nagani oil field.....	12
Fig. 7 Screening for EOR method based on API gravity (7).....	15
Fig. 8 EOR processes - classification and methods .....	17
Fig. 9 Factors upon which the main types of enhanced oil recovery methods act <sup>(6)</sup> .....	18
Fig. 10 Laboratory measurements of the dead oil viscosity .....	21
Fig. 11 Improvement in areal sweep efficiency by use of polymer – (a) unfavorable mobility ratio; (b) favorable mobility ratio; <sup>(6)</sup> .....	25
Fig. 12 Change into viscosity for the polymer sample with apparent viscosity closer to the oil's.....	26
Fig. 13 Crossflow effect in polymer flood of layered reservoir <sup>(6)</sup> .....	26
Fig. 14 Location of the main types of polymer retention in the porous media flow <sup>(6)</sup> .....	27
Fig. 15 Structure of HPAM (Aluhwal and Kalifa 2008) (13) .....	28
Fig. 16 Plot of the relative permeability ratio over the water saturation .....	31
Fig. 17 Plot of the $f_w$ and $df_w/dS_w$ vs. $S_w$ regarding the waterflooding .....	32
Fig. 18 Graphical evaluation of the water saturations located behind the breakthrough due to the waterflooding .....	33
Fig. 19 Water saturation profile as a function of distance (feet) and time (days) .....	36
Fig. 20 Reservoir performance due to the waterflooding.....	40
Fig. 21 Plot of the $f_w$ and $df_w/dS_w$ vs. $S_w$ for polymer-augmented waterflooding .....	41
Fig. 22 Graphical evaluation of the water saturations located behind the breakthrough due to the polymer-augmented waterflooding.....	42
Fig. 23 Polymers front profile as a function of distance (feet) and time (days).....	44
Fig. 24 Reservoir performance due to the polymer augmented waterflooding .....	47
Fig. 25 Comparison of the results received from waterflooding and vicious flooding: with the green line is depicted the improved field oil production rate (FOPR) due to the increased viscosity and with red line is depicted FOPR due to water flooding. ....	50
Fig. 26 Change into reservoir pressure due to the injection of high viscous brine compared with the water injections: with the green line is depicted improved reservoir pressure (RPR) due to the increased viscosity and with the red line is depicted RPR due to water flooding.....	51

## Bibliography

1. **Grubb, Adam.** Peak Oil Primer. *Resilience*. [Online] Oct 20, 2011. [Cited: 03 30, 2014.] <http://www.resilience.org/primer>.
2. **Capron, Jerome Sevin and Baptiste.** Seizing the EOR Opportunity. *Schlumberger*. [Online] 2014. [Cited: 04 01, 2014.] [http://www.sbc.slb.com/Our\\_Ideas/Energy\\_Perspectives/2nd%20Semester13\\_Content/2nd%20Semester%202013\\_Seizing.aspx](http://www.sbc.slb.com/Our_Ideas/Energy_Perspectives/2nd%20Semester13_Content/2nd%20Semester%202013_Seizing.aspx).
3. Norwegian Petroleum Directorate. *Norwegian Petroleum Directorate*. [Online] 06 29, 2009. [Cited: 03 29, 2014.] <http://www.npd.no/en/Topics/Improved-Recovery/Temaartikler/Why-do-we-not-recover-100-per-cent-of-the-oil/>.
4. **Abdus Satter, Ph.D., Ghulam M. Iqbal, Ph.D., P.E., James L. Buchwalter, Ph.D., P.E.** *Practical enhanced reservoir engineering Assisted with simulation software*. Tulsa : PennWell Corporation, 2008.
5. **Ahmed, Tarek.** *Reservoir engineering Handbook Third edition*. Burlington : Elsevier, 2006.
6. **Baviere, M.** *Basic concepts in enhanced oil recovery processes Critical reports on applied chemistry volume 33*. s.l. : Elsevier science, 1991. 1-85166-617.
7. *EOR Screening Criteria Revisited - Part 1: Introduction to Screening Criteria and Enhanced Recovery Field Projects*. **J.J. Taber, SPE, F.D. Martin, SPE, and R.S. Seright, SPE, New Mexico Petroleum Recovery Research Center**. s.l. : SPE Reservoir Engineering, August 1997.
8. Wikipedia - API gravity. *Wikipedia - API gravity*. [Online] March 30, 2014. [Cited: April 26, 2014.] [http://en.wikipedia.org/wiki/API\\_gravity](http://en.wikipedia.org/wiki/API_gravity).
9. **Af Abdus Satter, Ghulam M. Iqbal, James L. Buchwalter.** *Practical Enhanced Reservoir Engineering: Assisted with Simulation Software*. Oklahoma : PennWell, 2007.
10. *Estimating the Viscosity of Crude Oil Systems*. **H. D. Beggs, SPE-AIME, J. R. Robinson**. Tulsa, Okla. : JOURNAL OF PETROLEUM TECHNOLOGY, 1978. SPE 5434.
11. *Reservoir Engineering for Geologists Part 3 – Volumetric Estimation*. **Lisa Dean, Fekete Associates Inc.** DECEMBER 2007.
12. **Ahmed, Tarek.** *Reservoir Engineering Handbook Fourth edition*. s.l. : Elsevier, 2010. 978-1-85617-803-7.
13. **Green, Don W. Willhite, G. Paul.** *SPE Textbook Series, Volume 6 : Enhanced Oil Recovery*. Richardson, TX, USA : Society of Petroleum Engineers, 1998. 9781613991619 .
14. **Yongpeng Sun, Laila Saleh and Baojun Bai.** Measurement and Impact Factors of Polymer Rheology in Porous Media. [book auth.] Dr. Juan De Vicente. *Rheology*. s.l. : InTech, 2012.

15. **william C. Lyons, Gary J. Plisga.** *Standard handkook of Petroleum and Naturalgas engineering, Second Edition.* Burlington : ELSEVIER, 2005. 0-7506-7785-6.
16. *Polymers for enhanced oil recovery:A paradigm for structure-property relationship in aqueous solutio.* **D.A.Z. Wever, F. Picchioni, A.A. Broekhuis.** s.l. : Elsevier, 2011, Vol. Progress in polymer science 36.
17. *Network models for two-phase flow in porous media Part 1. Immiscible microdisplacement of non-wetting fluids.* **Madalena M. Dias, Alkiviades C. Payatakes.** Great Britan : s.n., 1986.
18. **Dr. Larry W. Lake, Dr. Mark P. Walsh.** *Enhanced oil recivery (EOR) field data litherature search - TECHNICAL REPORT.* Austin : Department of Petroleum and Geosystems Engineering University of Texas at Austin, 2008.
19. *Reservoir Management for Waterfloods—Part II.* **Baker, Richard.** Canada : The Journal of Canadian Petroleum Technology, 1998, Vol. 37.
20. *NEW VISCOSITY CORRELATIONS FOR DEAD CRUDE OILS.* **M. Sattarina, H. Modarresi, M. Bayata, M. Teymorria.** s.l. : Petroleum & Coal, 2007. 1335-3055.